

# Helical organization of tropical cyclones

G V Levina<sup>1,2</sup>

<sup>1</sup> Institute of Continuous Media Mechanics, Ural Branch of the Russian Academy of Sciences, Akademik Korolyov Street, Perm 614013, Russia

<sup>2</sup> Space Research Institute, Russian Academy of Sciences, Moscow, Russia

E-mail: levina@icmm.ru

**Abstract.** In this work we consider a helical flow organization on small and large space scales in a forming tropical cyclone and offer a quantitative analysis for early stages in evolution of large-scale helical vortex based on diagnosis of a set of integral helical and energetic characteristics. Using the data from a near cloud-resolving numerical simulation by Regional Atmospheric Modeling System (RAMS), a key process of vertical vorticity generation from horizontal components and its amplification by special convective coherent structures - Vortical Hot Towers (VHTs) - is highlighted. The process is found to be a pathway for generation of a velocity field with linked vortex lines of horizontal and vertical vorticity on local and system scales. This reveals itself in generation of nonzero and increasing integral helicity of the vortex system during tropical cyclone formation. Based on these results, a new perspective on the role of VHTs in the amplification of the system-scale circulation is emphasized. They are the connectors of the primary tangential and secondary overturning circulation on the system scales and are elemental building blocks for the nonzero system-scale helicity of the developing vortex throughout the tropical cyclone evolution from genesis to the mature hurricane state. Calculation and analyses of helical and energetic characteristics together with hydro- and thermodynamic flow fields allow the diagnosis of tropical cyclogenesis as an event when the primary and secondary circulations become linked on system scales.

## 1. Introduction.

Tropical cyclones in the Earth's atmosphere are between the most dangerous and mighty weather events. Despite considerable efforts and achievements of modern science their genesis remains between the most intricate enigmas of meteorology as well as no a clear consensus of opinion has yet emerged concerning ways of the post-genesis vortex amplification up to a hurricane intensity and physical mechanisms contributing to it.

There appears, however, a growing consensus in hurricane investigators' community that deep cumulonimbus convection of 2-20 km horizontal scales, which transfers sensible and latent heat from the underlying surface throughout the troposphere layer in the tropics, represents the main mechanism to intensify a pre-existing cyclonic circulation on the atmospheric mesoscales ( $\sim 200$  km) to a vortex of hurricane strength (Ritchie and Holland, 1997; Simpson et al., 1997; Emanuel, 2003). One can find more studies concerned with examining the role of cloud convection (however, without consideration of its helical features) in tropical cyclone formation.

On this background a revolutionary paradigm (Hendricks et al., 2004; Montgomery et al., 2006; Montgomery and Smith, 2010) appeared and is rooting in tropical cyclone investigations which allows explaining on an unified basis both genesis and intensification stages. The

paradigm is based on a fundamental idea of self-organization which is applied to moist convective turbulence in the tropical atmosphere. The observed process of self-organization highlights a key role of special coherent structures, so-called vortical hot towers, in a whole evolution of tropical cyclone (Montgomery and Smith, 2010). The self-organization is realized via convective structure mergers, which are accompanied by an upscale vorticity growth.

The hot towers in the tropical atmosphere of the Earth were first described by Riehl and Malkus (1958) as horizontally small but intense cumulonimbus convection cores that reached the tropopause, that in the tropics typically lies at least 15 km above sea level, via nearly undilute ascent and essentially contributed into the vertical heat transport and mass flux of the tropical overturning circulation (Hadley cell).

Recently, in numerical simulations (Hendricks et al., 2004; Montgomery et al., 2006) “vortical” hot towers (VHTs) were found and argued as the preferred mode of convection in tropical cyclones. As it was noted by Molinari and Vollaro (2010), VHTs are helical by definition because they contain coincident updrafts and vertical vorticity. The contemporaneous tropical meteorology, (see, e.g., the Glossary by Dunkerton et al. (2009)), considers the vortical hot towers in pre-storms conditions as “deep moist convective clouds that rotate as an entity and/or contain updrafts that rotate in helical fashion (as in rotating Rayleigh-Bénard convection). . . . These locally buoyant vortical plume structures amplify pre-existing cyclonic vorticity by at least an order of magnitude larger than that of the aggregate vortex.”

The vortical hot towers have been identified as fundamental coherent structures in both the tropical cyclone genesis process (Hendricks et al., 2004; Montgomery et al., 2006; Braun et al., 2010; Fang and Zhang, 2010) and the tropical-cyclone intensification process (Nguyen et al., 2008; Shin and Smith, 2008; Montgomery et al., 2009; Montgomery and Smith, 2010).

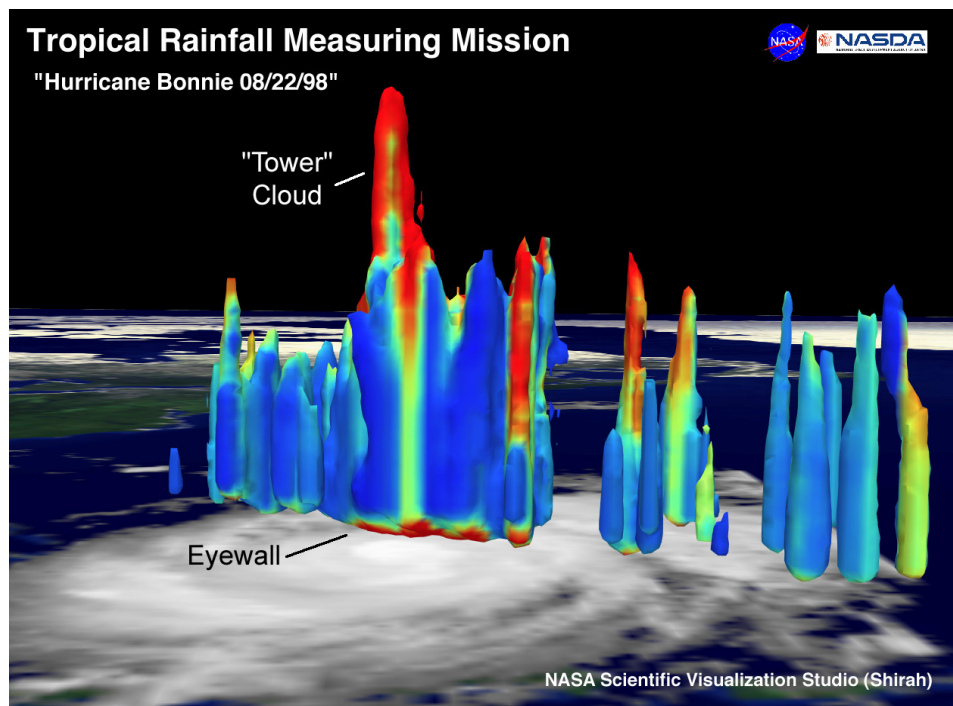


**Figure 1.** Hot Towers in Hurricane Bonnie 1998. Altitude of clouds is exaggerated. Borrowed from (Wikipedia, 2012).

An overview of modern knowledge on VHTs including observational evidence for vortical turbulent convection in pre-storms can be gained in a recent review-report by Montgomery and Smith (2010).

As it has been shown in detail by idealized near-cloud-resolving numerical simulations by Montgomery et al. (2006), within the cyclonic vorticity-rich environment of the mesoscale convective vortex (MCV) embryo the self-organization of initially generated small-scale convective updrafts started since the very first hours of vortex evolution, spawned deep cumulonimbus towers possessing intense cyclonic vorticity in their cores (VHTs) and was crowned with formation of mesoscale tropical depression vortex. During all subsequent stages of vortex intensification from the tropical depression up to the mature hurricane strength, a number of VHTs of different scale and strength were always observed within the vortex circulation. The work clearly demonstrated how an intense mesoscale long-lived vortex could develop from cumulonimbus convective turbulence as a result of system-scale convergence and upscale vorticity growth, be sustained and intensified further in favorable ambient conditions.

The paper is organized as follows. In Section 2 special features of helical turbulence, which can result in generation of large-scale vortex instability, are discussed; a longstanding theoretical hypothesis on the turbulent vortex dynamo that was introduced to explain a process of intense large-scale vortices formation in planet atmospheres is revisited, and a recent numerical approach designed to identify such large-scale instability during tropical cyclone development in the Earth's atmosphere is briefly reminded. In Section 3 helical peculiarities of tropical cyclone formation are examined, the problem formulation is given to investigate helical self-organization of moist convective atmospheric turbulence by use of RAMS (Regional Atmospheric Modeling System) simulation and its numerical realization is described, and finally, a simple test undertaken to compare our computed helicity field in tropical cyclones with estimations of other investigators is discussed as well. Sections 4–6 concern new insights in tropical cyclone formation based on the concept of helicity. In Section 4 we discuss global factors that contribute initially to inhomogeneity of atmospheric turbulence and helicity generation. Section 5 presents a quantitative analysis and discussion of how helicity is generated on cloud convection scales. Based on advanced ideas, quantitative pinpointing of key events in tropical cyclone evolution, namely, tropical cyclone genesis and tropical depression formation, is performed in Section 6. Section 7 summarizes the main findings.

## **2. Special features of turbulence lacking the mirror symmetry**

It is useful at this juncture to recall the long-standing classical concept of turbulent flows, in which any large-scale flow structure, for instance a vortex of spontaneous or forced origin, should be destroyed by turbulence, as the developed turbulence tends to restore the broken symmetry (Monin and Yaglom, 1975). Homogeneity or isotropy of turbulence that is violated on large scales is generally recovered on smaller scales, as it follows the Kolmogorov-Obukhov local theory (Kolmogorov, 1941; Obukhov, 1941), and disturbance decay due to turbulent viscosity is accompanied by the energy transfer from the large-scale motion to small-scale turbulent pulsations. Under these conditions the existence of long-lived structures in which the spatial dimension which essentially exceeds the turbulence scale seems to be hardly probable.

### *2.1. Helicity of the velocity field*

It would be quite another matter if the broken symmetry can not be restored by turbulence. Such might be the case with the lack of reflection symmetry (mirror-invariance breakdown) which is compatible with the theory of local structure of turbulence. Fluid motions exhibiting this property are called helical and described mathematically by a quantity, which is well-known in fluid dynamics as helicity of the velocity field (Moffatt, 1969). This quantity is defined as

the dot product of velocity  $\mathbf{V}(\mathbf{r}, \mathbf{t})$  and vorticity  $\mathit{curl}\mathbf{V}(\mathbf{r}, \mathbf{t})$  vectors (see, e.g., review articles by Moffatt and Tsinober (1992); Levina et al. (2000) and references therein on helicity and helical turbulence, and the more recent paper by Pouquet and Mininni (2010)). The volume integral calculated in a specific space domain

$$H = \int \mathbf{V} \cdot \mathit{curl}\mathbf{V} d\mathbf{r} \quad (1)$$

gives the total (or global) helicity of vortex system, where  $\mathbf{V} \cdot \mathit{curl}\mathbf{V}$  is the helicity density of the flow. Both quantities are pseudoscalars, i.e., they change sign under change from a right-handed to a left-handed frame of reference (Moffatt and Tsinober, 1992).

A non-vanishing volume-integral of helicity,  $\langle H \rangle \neq 0$ , implies the symmetry break of turbulence with respect to coordinate system reflections (Moffatt, 1978; Frisch, 1995). The mean helicity, like energy, is an inviscid quadratic constant of motion in barotropic fluids. Existence of the second quadratic constant of motion (in addition to the energy) makes helical flows relatively more stable. Helical structures resist dissipation and survive longer (Lilly, 1986).

However, unlike energy the helicity can be both positive and negative. Its sign determines the predominance of the left-handed or the right-handed spiral motions in the examined flow. If we choose a right-handed Cartesian or orthogonal curvilinear frame for our further consideration, positive mean helicity will be generated in the moist atmosphere under the predominance of cyclonic updrafts and/or anticyclonic downdraft motions. Similarly, negative helicity will be generated for the case of anticyclonic updrafts and/or cyclonic downdraft flows.

Helicity is one of the most important characteristics for describing the structure of vortex fields. This quantity is a topological invariant, which measures the degree of linkage of the vortex lines (Moffatt, 1969, 1978; Moffatt and Tsinober, 1992; Frisch, 1995). This fundamental meaning of helicity, which the subsequent discussion of our main results will be centered round, was recalled and highlighted in our recent paper (Levina and Montgomery, 2011).

Let us only reproduce here a picture (Figure 2) given by Moffatt (1969), namely, Figure 1 of his paper as a simple illustration for this complex topological notion.

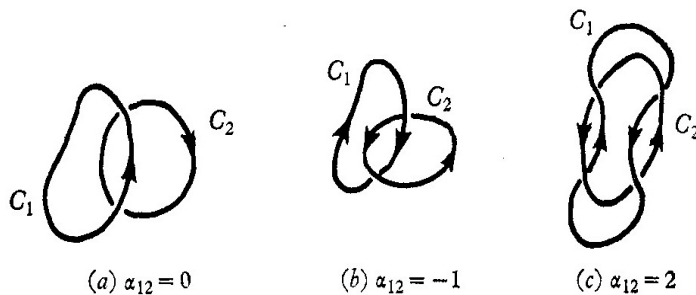


**Figure 2.** The degree of linkage of two closed filaments  $C_1, C_2$  (where  $\alpha_{12}$  is the “winding number” of the curves  $C_1$  and  $C_2$ ). The choice of sign in (b), (c) is determined by the relative orientation of the two filaments. Borrowed from (Moffatt, 1969).

Obviously, a real three-dimensional vortex field can have both linked and knotted vortex lines, and in a repeated manner. However, it is described and illustrated (Moffatt, 1969; Moffatt and Tsinober, 1992), how an arbitrary vorticity field can be decomposed into a number of simpler fields of trivial topology, and a knotted vortex line may be decomposed into two (or more) linked but unknotted vortex lines by the insertion of a pair (or pairs) of equal and opposite vorticity segments.

## *2.2. Large-scale instabilities in helical turbulence*

In the theory of turbulence there exists a fundamental hypothesis about a small-scale helical turbulence that under certain conditions may evoke a large-scale instability governing the structure formation. The sources of helical turbulence are known to be the force fields of a pseudovector nature, such as magnetic or Coriolis force fields.

The specific properties of small-scale helical turbulence resulted in large scale structure generation were first discovered in magnetohydrodynamics (Steenbeck et al., 1966). This phenomenon is known as the alpha-effect. The first theoretical example of large-scale helical instability in general (non-MHD) hydrodynamics was proposed by Moiseev et al. (1983a) and, by analogy, coined the hydrodynamic alpha-effect. As it has been shown, helicity influences the mean flow fields through the Reynolds stress tensor.

It is very important to note that in both, MHD and non-MHD, cases the theory gives thresholds for the generation of large-scale “helical” instability.

Since the very first theoretical studies on helicity and helical turbulence had appeared in the 1960s, a great number of numerical investigations of helical features of turbulence were undertaken in both general fluid dynamics and magnetohydrodynamics. Thus, a recent work by Pouquet and Mininni (2010) would be recommended to gain a view on the problem and knowledge on modern high spatial resolution numerical simulations, up to  $1536^3$ , which were carried out in National Center for Atmospheric Research (NCAR). In their motivation the authors (Mininni et al., 2009; Mininni and Pouquet, 2010a,b; Pouquet and Mininni, 2010) referred to the important role that helicity played in geophysical and astrophysical flows. Specifically, a forcing function used in (Mininni and Pouquet, 2010a,b; Pouquet and Mininni, 2010) was a fully helical flow that could mimic the effect of atmospheric convective motions. That function injected both energy and helicity in the flow. As we know, in a real atmosphere there exist natural ways for helicity generation, for instance, by interaction of rotation and stratification (Moffatt, 1978) or in the Ekman’s boundary layer (Koprov et al., 2005).

In simulations (Mininni et al., 2009; Mininni and Pouquet, 2010a,b; Pouquet and Mininni, 2010), an inverse energy cascade from small-scale motions to large-scales ones was found in the presence of rotation. The inverse energy transfer was accompanied by merging of small-scale helical vortices. As a result, the characteristic width of structures in the energy density field increased. This strongly reminds us the atmospheric scenario of the “vortical hot tower route to tropical cyclogenesis” observed by Montgomery et al. (2006).

An important summarizing remark made in (Pouquet and Mininni, 2010) about the interplay between rotation and helicity is well-accordant to our own sight of the problem in that the former breaks the mirror symmetry of the turbulence and the latter quantifies flow departures from the symmetry.

In the most recent paper by Biferale et al. (2012), it was discovered that all three-dimensional flows in nature possess a subset of nonlinear evolution leading to a reverse energy transfer: from small to large scales. Based on numerical investigations of Navier-Stokes equations, the authors showed the existence of inverse energy cascade in three-dimensional fully isotropic turbulent flows when mirror symmetry was broken. This means that the inverse energy flux may be found in a broad range of flows.

All above cited investigations impel us to advert to theoretical works by Moiseev et al. (1983a,b) who anticipated these recent findings a long ago.

## *2.3. A hypothesis on the turbulent vortex dynamo*

Nearly thirty years ago in paper (Moiseev et al., 1983b), a hypothetical scenario for intensification and sustaining of large-scale vortex disturbances in the atmosphere due to energy transfer from small-scale helical convective turbulence – the so called turbulent vortex dynamo – was proposed as a possible illustration for self-organization of turbulence with the broken mirror symmetry.

The theoretical estimates obtained by substituting the specific atmospheric parameters in solutions (Moiseev et al., 1983b) were tested to describe tropical cyclone formation in the Earth's atmosphere (Moiseev et al., 1983b) as well as, a few years later, to explain the size and structure of large-scale long-lived vortex disturbances in Jovian atmosphere after the collision of comet Shoemaker-Levy 9 with Jupiter in July 1994 (Fortov et al., 1996; Ivanov et al., 1996). The theory showed a very good agreement with the characteristics of observed phenomena in the atmospheres of both planets. Summary of those results was given in a review work by Levina et al. (2000).

A probable physical scenario for the helical self-organization (Moiseev et al., 1983a,b; Levina et al., 2000) supposed an initial break of the mirror symmetry of turbulence, for example, due to a weak large-scale vortex disturbance. That is well consistent with the problem formulation in (Montgomery et al., 2006), where simulations started with a pre-cursor mesoscale cyclonic vortex. The incipient process of helical self-organization would have to reveal itself in the non-zero mean helicity generation and consequent increasing of its level. Large helicity should suppress the energy flux to the scale of dissipation due to weakening of nonlinear interactions (Lilly, 1986), thereby favoring an energy accumulation in the inertial range, and then its transfer to larger scale motions. In this connection, an inverse cascade or nonlocal energy transfer was expected to exist for developed helical turbulence. In flow patterns such process could reveal itself as a merging of small-scale turbulent cells to organize larger scale structures.

As a sign that could help to precisely identify genesis of large-scale atmospheric vortex one envisioned to have an emerging linkage of the system-scale primary (tangential) and secondary (overturning/transverse) circulation in a forming vortex structure. A schematic of such linkage is shown in Figure 2. The authors (Moiseev et al., 1983a,b; Levina et al., 2000) anticipated that the linkage should result in a “helical” feedback between the system-scale circulations that would mean a mutual intensification of both circulations due to energy influx from small-scale moist convective helical turbulence. The initiation of such helical feedback would make the forming large-scale vortex energy-self-sustaining. Thus, the time moment corresponding to the feedback emergence could be considered as the genesis event for a tropical cyclone.

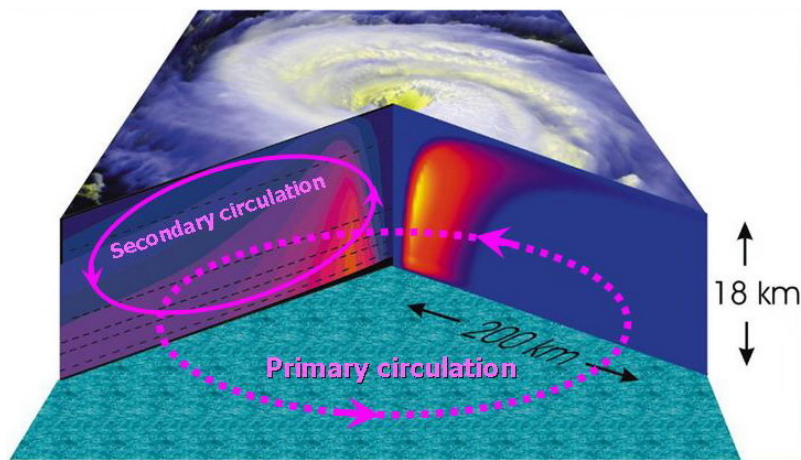


**Figure 3.** Schematic of the linkage of primary and secondary circulation is superimposed on a cutaway of composite tropical cyclone borrowed from (Emanuel, 2003).

Later, processes of vorticity and helicity generation in the moist rotating turbulent atmosphere were theoretically examined by Kurgansky (1993, 1998, 1999) who showed that an energy release due to phase transition of moisture was the necessary condition required to

achieve the non-zero dynamo-effect. These investigations were summarized in section 4.1 of Kurgansky's book (2002).

Thus, a number of factors have been identified which seem to be responsible for helicity generation and the possibility of turbulent vortex dynamo in the inhomogeneous atmosphere: rotation of the atmospheric layer, developed moist convective turbulence and internal heat release due to phase transitions of moisture.

#### *2.4. Numerical approach to identify the large-scale helical instability in the atmosphere*

A numerical approach for investigation of large-scale helical instability in the atmosphere was developed by Levina et al. (2004); Levina (2006), Levina and Burylov (2006; hereafter L06), and first tested in a simpler case, namely, to simulate helical-vortex effects in laminar Rayleigh-Bénard convection by use of an additional helical force.

The applied helical forcing had a physical interpretation. The function had the identical tensor structure with the generating alpha-term in the mean-field velocity equation describing the turbulent vortex dynamo in a convective system (Moiseev et al., 1988; Rutkevich, 1993; Levina et al., 2000). So long as the alpha-term in the cited works (following the statement of those problems and procedure of averaging under developing the mean-field equation) parameterized the influence of small-scale helical turbulence generated in a rotating fluid with internal heat release, thereby, providing us with an additional energy flux from smaller to larger scales, so did the forcing and simulated these effects.

Numerical investigations carried out in (Levina, 2006; L06):

- gave a vivid example of non-zero mean helicity,  $\langle H \rangle \neq 0$ , generation that implied the broken mirror symmetry,
- demonstrated new effects in flow structure and energetics attributed to a large-scale instability,
- confirmed a threshold type onset of this new helical instability,
- highlighted the generation of positive helical feedback between the tangential and overturning circulation in a vortex system,
- demonstrated how the helical feedback could be identified by examining integral kinetic energies of the tangential and overturning circulation,
- showed a probable scenario for development of the instability by merging of helical convective cells and consequent intensification of newly forming larger-scale helical vortices,
- emphasized the crucial role of vertical flow component in the whole scenario of new instability,
- pointed out an increased effectiveness of heat transfer within a helical (!) and larger vortex flow configuration.

These findings gave the authors of (Levina, 2006; L06) an impetus to search for possible application to tropical cyclone investigations.

### **3. Examination of the helical peculiarities of tropical cyclone (TC) formation**

The term “helical cyclogenesis” was still introduced by Levich and Tzvetkov (1984), who suggested a leading role of helicity fluctuations (when mean global helicity vanished) to provide an inverse energy cascade in three-dimensional turbulence. An extended discussion was carried out in their later reviewing work (Levich and Tzvetkov, 1985) about how the proposed mechanism could work enabling formation of mesoscale atmospheric phenomena such as tropical cyclones, subtropical hurricanes, polar lows. It is worth noting that Levich and Tzvetkov (1984, 1985) hypothesized quite differently of Moiseev et al. (1983a,b), where the non-zero mean global helicity generation was considered as a necessary condition for large-scale intense vortex structures formation in the atmospheric turbulence.

Despite the above mentioned long standing theoretical hypotheses on the role of helicity in tropical cyclogenesis, helical features of the velocity field have not been highlighted in real tropical cyclone investigations until very recently.

As far as we are aware, besides our own works (Levina and Montgomery, 2010, 2011) and a number of conference proceedings in 2009-2012, which introduced helicity to articulate our point of view on tropical cyclone formation as self-organization of moist convective atmospheric turbulence with the broken mirror symmetry, only papers (Molinari and Vollaro, 2008, 2010; Nolan, 2011) can be consistent with purposes of our present study. The investigations by Molinari and Vollaro (2008, 2010); Nolan (2011) include calculations and analysis of storm relative environmental helicity (SREH) that was introduced (Davies-Jones et al., 1990) as a vertical integral of the helicity in the lower troposphere (most often for 1, 3, or 6 km layer in height). This quantity was substantiated and applied very successfully to predict the likelihood of mid latitudes severe storms (Lilly, 1986; Davies-Jones et al., 1990; Johns and Doswell, 1992; Droegemeier, 1993; Rasmussen and Blanchard, 1998; Weisman and Rotunno, 2000).

To motivate their research goals, Molinari and Vollaro (2008, 2010) presented a comprehensive review on helicity studies connected with its role in stabilizing strong convective storms in mid latitudes as well as cited a few works on similar intense vortices observed in tropical cyclones over water (Bogner et al., 2000) and after landfall (McCaul, 1987, 1991). An analysis of helicity was performed (Molinari and Vollaro, 2008, 2010) in the context of its possible role in increasing the ability of developing hurricane to resist the negative impact of the ambient vertical wind shear. Helicity was calculated using tropospheric-deep dropsonde soundings carried out by reconnaissance aircrafts under investigations of eight tropical cyclones of 1998-2001 seasons during wide-ranging campaign CAMEX (Convection and Moisture Experiment) (Kakar et al., 2006) organized by NASA (National Aeronautics and Space Administration). The authors hypothesized in both papers that the long-lived convective cells which arise as a consequence of the extreme helicity combined with moderate but sufficient convective available potential energy (CAPE) enable the storm to resist the impact of the shear. If in the first paper it was argued that the existence of intense cells might help the Hurricane Bonnie (1998) maintaining its intensity when ambient 850-200 hPa vertical shear remained near  $12.5 \text{ m s}^{-1}$ , then the second paper gave all eight considered storms categorized (from the abstract) “as having large or small shear, with  $10 \text{ m s}^{-1}$  as the dividing line”. The conclusion was made that supercells were more likely to occur in storms experiencing large ambient shear.

Extreme values of helicity, among the largest ever reported in the literature, were found in the vicinity of deep convective cells and vortical hot towers (Molinari and Vollaro, 2008). When discussing a role of individual cells in tropical cyclones in the context of helicity, Molinari and Vollaro (2010) noted the evident helical nature of vortical hot towers.

Nolan (2011) examined SREH within his new approach “Method of Point-Downscaling” proposed to determine the favorableness for tropical cyclone development of an atmospheric environment, where the term “development” was used as referred to both tropical cyclogenesis and the early intensification of a tropical cyclone after genesis. Based on results (Molinari and Vollaro, 2008, 2010) that large values of low-level helicity are favorable for the emergence of intense and long-lasting rotating convective cells in tropical cyclones, the author considered the concept of helicity to explain the effect of environmental wind profiles that turned with height on tropical cyclone development. Simulations carried out with idealized wind profiles showed that a “clockwise” turning hodograph was much more favorable for development than a “counterclockwise” turning hodograph.

As the above review shows, there exist only a few works which address helicity in tropical cyclones formation. Amongst them, in the context of the upscale self-organization of moist convective atmospheric turbulence only our own investigations were carried out in the current millennium.

Only recently has it become possible to address examination of the hypothesis on turbulent vortex dynamo in the tropical atmosphere of the Earth with a physically consistent data set. And only recently have studies been conducted to examine reasonably high horizontal resolution ( $\sim 1$ - $3$  km of horizontal scale and less) numerical simulations of tropical cyclone formation that possess an adequate representation of both the deep cumulus and stratiform stages. Between these works Montgomery et al. (2006; hereafter M06) proposed a new scenario of hurricane formation based on self-organization of convective processes within a kinematically and thermodynamically favorable environment of a mesoscale convective vortex.

### *3.1. A vortical hot tower route to tropical cyclogenesis*

In M06, Montgomery and co-authors by using near-cloud-resolving simulations demonstrated how a mesoscale tropical depression (TD) vortex could develop from cumulonimbus convection as a result of system-scale convergence and upscale vorticity growth. Within the cyclonic vorticity-rich environment of the mesoscale convective vortex (MCV) embryo, the numerical simulations indicated that deep cumulonimbus towers possessing intense cyclonic vorticity in their cores, vortical hot towers (VHTs), emerged as the preferred coherent structures. The VHTs acquired their vertical vorticity through a combination of tilting of MCV-horizontal vorticity and stretching of MCV and VHT-generated vertical vorticity. Horizontally localized and exhibiting convective lifetimes on the order of one hour, VHTs overcame the detrimental effects of downdrafts by consuming convective available potential energy in their local environment, humidifying the middle and upper troposphere, and undergoing diabatic vortex merger with neighboring towers. In those simulations the growth of flow scales occurred by both system convergence and multiple diabatic vortex mergers alongside the more familiar dry adiabatic vortex merger of convectively generated remnants. The generated VHTs, each of 10-30 km horizontal scale, eventually resulted in an intense helical vortex, TD, on the atmospheric mesoscale. A number of VHTs always existed within the vortex circulation during further evolution of developing tropical cyclone.

Although helical features of these simulated flows were not taken into consideration within the framework of paper M06, self-organization of vortical convection was observed similar to “helical” scenario L06, namely, as an enlargement of vortex structures from the size of individual rotating cumulus clouds in the model, their induced concentration of absolute angular momentum on the system scale circulation, and their merging with each other to yield newly forming larger vortices and an intensifying circulation on the system scale.

Results of works L06 and M06 were brought in together and gave a start to introducing the analysis of helical characteristics of the velocity field in numerical investigations of tropical cyclones by use of atmospheric modeling systems.

In paper (Levina and Montgomery, 2010), the first investigation of tropical cyclone formation was conducted from the perspective of helical features of atmospheric flows of different scales, which contributed to the organization of the cyclone. Using the data M06, helical characteristics of the velocity field were calculated and analyzed. It has been discovered that the process of hurricane formation is accompanied by the generation of nonzero mean helicity in moist convective atmospheric turbulence that implies a new topology of the flow when it is characterized by linked vortex lines (Moffatt, 1969).

It is important to point out that no external assumptions are imposed on the fluid motions in our investigations. This means that no any forcing terms like that one applied in previous works (Levina, 2006; L06) were used to mimic a “helical alpha effect” in (Levina and Montgomery, 2010, 2011) as well as in the present paper. In other words, the obtained results are the outcome of a direct numerical simulation subject to the usual caveats of a sub-grid scale closure that was used to remove small scale motions at the horizontal grid scales of the model ( $\sim 3$ km).

This work is focused on the pivotal contribution of the helical flow topology on local and

system scales to interpreting the hurricane formation as a manifestation of the fundamental process of self-organization of turbulence that is implemented in the tropical atmosphere of the Earth as the vortical hot tower route to tropical cyclone genesis and intensification.

### 3.2. Numerical realization

In the present paper, ideas and methods proposed in (Levina (2006), L06), about which the corresponding discussion was given in section 2.4, are applied to post-processing of velocity fields obtained in (M06) by use of the numerical meteorological model RAMS (Regional Atmospheric Modeling System) developed at Colorado State University. Detailed information on the governing equations of hydro-thermodynamics of the atmosphere, parameterizations of turbulent processes, specific characteristics of the RAMS model configuration, initial and boundary conditions is given in paper (M06) as well as references to corresponding works.

Let us note further a number of features of numerical realization applied in (M06) that are of crucial importance for the problem under consideration.

The velocity fields used for calculations of helical and integral characteristics in this work were obtained in (M06) by use of the three-dimensional non-hydrostatic numerical modeling system comprising time-dependent equations for all three components of velocity (including the vertical one, see section 2.4 on its importance; and with taking into account the planetary rotation), pressure, potential temperature, total water mixing ratio, and cloud microphysics.

RAMS utilizes an interactive multiple nested grid scheme which allows explicit representation of cloud-scale features within the finest grid while enabling a large domain size to be used, thereby minimizing the impact of lateral boundary conditions. For all numerical experiments in (M06) three nested grids were used. For experiment A1 (see Table 1 that enumerates a part of numerical experiments from (M06) which are under consideration in this paper) the horizontal grid increments were 24 km, 6 km and 2 km, with  $(x, y, z)$  dimensions of  $64 \times 64 \times 26$ ,  $90 \times 90 \times 26$ , and  $137 \times 137 \times 26$ , respectively. For all other experiments analyzed here, increments and dimensions were 36 km, 9 km and 3 km, and  $40 \times 40 \times 26$ ,  $62 \times 62 \times 26$ , and  $92 \times 92 \times 26$ , correspondingly. Each nested grid was centered within the next coarsest grid. The vertical grid increment was 400 m at the surface and gradually stretched with height to the top of the domain at 22 km. The depth of the Rayleigh friction layer was 5 km.

A standard radiation boundary condition was used at the lateral boundaries, which assumes that disturbances reaching the boundaries move as linearly propagating gravity waves. A standard Rayleigh friction layer was included at upper levels in order to minimize reflection of gravity waves from the top of the model. All microphysical, radiative, and diffusive parameters were the standard ones employed for tropical summer conditions (M06). The initial temperature distribution in (M06) was the mean Atlantic hurricane season sounding which was representative of the so-called "non-Saharan-air-layer" air.

*3.2.1. Post-processing implementation* We performed calculations and analysis of helical and integral characteristics for six of nineteen numerical experiments (M06), which are presented in Table 1.

Post-processing of the model data was carried out on the finest computational grid for subsequent times with a time increment of 10 minutes during 72 hours of numerical experiment. Characteristics were calculated in the computational domain of  $276 \times 276 \times 20$  km<sup>3</sup>, at first, in Cartesian co-ordinates  $(x, y, z)$  by use of uniform finite-difference grid with increments  $\Delta x$ ,  $\Delta y$ ,  $\Delta z$ . Throughout the post analysis the vertical increment was identical and equal to 500 m; the horizontal increments were  $\Delta x = \Delta y = 3$  km, except experiment A1 with  $\Delta x = \Delta y = 2$  km.

We also applied an analysis of system-scale dynamics from a traditional vortex-centric perspective when the Cartesian model data were transformed into a local cylindrical coordinate

system. For these purposes we used the ‘‘Diagnostic Package’’ developed and described in (M06, Appendix B).

For the first 24 h of each simulation the center of the domain was utilized as the system-scale center. At later times, when the central vortex core started wandering off domain center due to convective asymmetries, the minimum horizontal wind speed at the lowest grid level was used to determine the center of circulation. The resulting center was kept constant with height. This approach is believed superior to using the location of minimum surface pressure because, at early times, the minimum surface pressure is typically found within VHT cores whose lifetimes are short (order 1 h) compared to the evolutionary time scale of the system-scale vortex.

The cylindrical grid used consisted of 25 azimuthal points. The number of radial points was dependent on the location of the vortex center. The radial grid spacing was uniform with a grid increment equal to the Cartesian horizontal grid spacing of the finest grid. Once a center was established, scalar fields were interpolated to the cylindrical grid. Vector fields, such as the radial and tangential wind components, were calculated by applying a rotation transformation to the Cartesian vector at each grid point. The tangential and radial velocities were then interpolated onto the cylindrical grid. Azimuthal averages were calculated as an arithmetic average of values along a constant radius, and are denoted with an overbar. Deviations from the azimuthal average are denoted with primes.

*3.2.2. Helical and integral characteristics* To analyze the process of self-organization of moist atmospheric convection observed under conditions of tropical cyclone formation as posed by (M06), a set of helical characteristics was computed, as well as some other integral characteristics of the velocity field which were applied in (Levina (2006), L06). The following characteristics were calculated with a time increment 10 min during the whole 72-hours evolution of tropical cyclone to obtain results discussed in this paper: three-dimensional relative helicity density

$$H_{i,j,k} = (\mathbf{V} \cdot \text{curl} \mathbf{V})_{i,j,k}, \quad (2)$$

as well as its two horizontal (and their resulting field) and vertical contributions separately

$$(H_x)_{i,j,k} = (V_x \cdot (\text{curl} \mathbf{V})_x)_{i,j,k}, \quad (3)$$

$$(H_y)_{i,j,k} = (V_y \cdot (\text{curl} \mathbf{V})_y)_{i,j,k}, \quad (4)$$

$$(H_x + H_y)_{i,j,k}, \quad (5)$$

$$(H_z)_{i,j,k} = (V_z \cdot (\text{curl} \mathbf{V})_z)_{i,j,k}, \quad (6)$$

two other important characteristics of the velocity field – enstrophy and kinetic energy densities:

$$\varepsilon_{i,j,k} = \frac{1}{2} (\text{curl} \mathbf{V})_{i,j,k}^2, \quad E_{i,j,k} = \frac{1}{2} (\mathbf{V})_{i,j,k}^2. \quad (7)$$

We calculated and took into examination mean (volume-integrated) values of helicity, enstrophy and kinetic energy integrated over the whole computational domain  $276 \times 276 \times 20 \text{ km}^3$  and normalized by number of grid points:

$$\langle H \rangle, \quad \langle \varepsilon \rangle, \quad \langle E \rangle, \quad (8)$$

and averaged values for their spatial contributions

$$\langle H_{hor} \rangle, \quad \langle H_{ver} \rangle, \quad (9)$$

$$\langle \varepsilon_{hor} \rangle, \quad \langle \varepsilon_{ver} \rangle, \quad (10)$$

$$\langle E_{hor} \rangle, \quad \langle E_{ver} \rangle. \quad (11)$$

Horizontal and vertical contributions averaged in both Cartesian and cylindrical coordinates were analyzed. Thus, in the above formulae a lower index “hor” refers to the full horizontal flow contribution – the sum of x- and y-contribution in the Cartesian coordinates and of radial and tangential field in the cylindrical case. To obtain azimuthal mean values the procedure applied in (M06) and described above was used in our current investigation.

### 3.3. A simple test for computed helicity field in TC

When developing and applying a new approach it is usually appropriate first to find a possibility and test newly obtained results by using some well-known data. For this purpose we were lucky to have paper by Molinari and Vollaro (2008), in which an estimate for helicity was found that allowed easy obtaining a similar characteristic within our approach.

In paper (Molinari and Vollaro, 2008), the authors introduced a number of helical characteristics including that one they called “total helicity”, however, its definition was quite different from that identical we use in this paper. Under given name they considered a helicity value, in which the terms involving the vertical motion in both the velocity and vorticity vectors were neglected similarly to midlatitude severe weather applications. In their case it was reasonable because they evaluated helicity from dropsonde sounding data and did not have estimates for vertical velocity. Thus, the resulting expression for such helicity value was (Lilly, 1986; Molinari and Vollaro, 2008)

$$H_{TOT} = \mathbf{V}_{hor} \cdot \left( \mathbf{k} \times \frac{\partial \mathbf{V}_{hor}}{\partial z} \right) = \mathbf{k} \cdot \left( \frac{\partial \mathbf{V}_{hor}}{\partial z} \times \mathbf{V}_{hor} \right), \quad (12)$$

where  $\mathbf{k}$  is the vertical unit vector and  $\mathbf{V}_{hor}$  is the horizontal velocity vector.

A few values of total helicity  $H_{TOT}$  were calculated, equivalent to a cell motion of zero for the 0-6 km layer in height (Molinari and Vollaro, 2008, Table A1). The highest value of  $H_{TOT} = 2578 \text{ m}^2 \text{ s}^{-2}$  was found in Hurricane Bonnie (1998) on August 24 when the maximum surface wind was about  $55 \text{ m s}^{-1}$ .

To compare our results with data of paper (Molinari and Vollaro, 2008) we calculated helicity (2) of two kinds integrated over 0-6 km height layer of unit square. The first of them (shown as “Total Helicity” in Fig. 4a) included vertical components of velocity and vorticity whilst we neglected the vertical motion completely in helicity of second kind (“SREH” given in Fig. 4b) as it has been done in (Molinari and Vollaro, 2008). The latter value is equivalent to SREH given by formula (3) in (Molinari and Vollaro, 2008) and calculated for cell motion of zero,  $\mathbf{c} = 0$ .

For helicity of both kinds maximal and minimal values over the computational domain at every time moment were found and analyzed together with other characteristics of velocity field. Evolution of maximal values of helicity during the whole experiment A2 time of 72 hours was plotted with a time increment equal to 10 minutes (Fig. 4a,b).

As we can see in Figure 4, maximal values of helicity are essentially higher when the vertical motion was not neglected (Fig. 4a). In this case total helicity is mainly found to be between  $2000\text{-}2400 \text{ m}^2 \text{ s}^{-2}$  during a time span 56-65 hours when the maximum surface wind is between  $33.5 \text{ m s}^{-1}$  and  $42.5 \text{ m s}^{-1}$ . Within this time interval total helicity reaches its highest value equal to  $2700 \text{ m}^2 \text{ s}^{-2}$ , which is even slightly higher than that found in (Molinari and Vollaro, 2008).

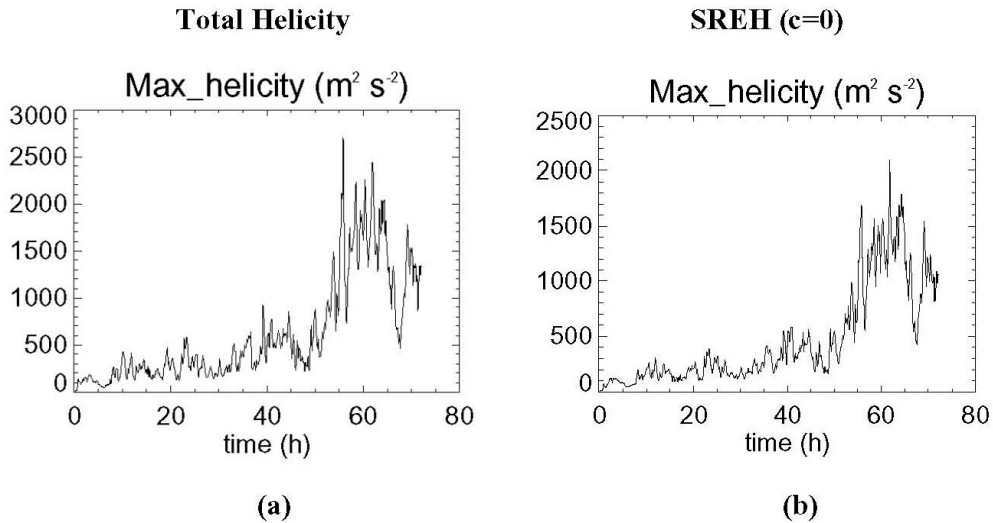


**Figure 4.** Maximal values of helicity integrated over 0-6 km height layer of unit square during 72 hours of TC evolution in Experiment A2: calculated with (a) and without (b) contribution of the vertical components of velocity and vorticity.

When the vertical flow is neglected (Fig. 4b), the highest helicity values are appreciably smaller, between 1500-1800  $\text{m}^2 \text{s}^{-2}$ , with a record value of 2100  $\text{m}^2 \text{s}^{-2}$ , and found to be reached within the same time interval from 56 to 65 hours of simulation, as in the previous case.

Thus, the undertaken testing supplied helicity values which are reasonably close to those ones found by Molinari and Vollaro (2008). Our results confirmed the existence of extreme values of helicity in TCs, which were first emphasized in (Molinari and Vollaro, 2008)

It was also found that there exists a big difference in helicity estimates with and without the vertical motion. As a result, it is worth noting that if one neglects the vertical motion in order to examine helicity when working with dropsonde sounding data it looks comprehensible. However, it does not so when we meet the similar approach applied for TC investigations by modern numerical simulation which could easily operate with all components of velocity. Probably, the latter approach keeps a tribute to deep-rooted traditions.

#### 4. TC formation: factors contributing initially to inhomogeneity of atmospheric turbulence and helicity generation

Following the summary of theoretical and numerical investigations given in Section 2, which highlights necessary conditions for large-scale instabilities in helical turbulence, and the statement of the problem for numerical simulation of TC formation in (M06) described in Section 3, we can note a number of factors which contribute to generation of turbulence inhomogeneity and helicity (i.e. the linkage of vortex lines) in the investigated atmospheric area of potential cyclogenesis from the very first beginning of numerical experiment as posed in M06.

The most common factors to generate them are the planetary rotation and thermal stratification (Moffatt, 1978). In a case of concurrent influence of both Coriolis force and buoyancy forces on the fluid, the rotation vector  $\boldsymbol{\Omega}$  and the gravity vector  $\mathbf{g}$  provide independent preferred directions which will affect the statistics of any turbulent field and create anisotropy of turbulence.

The interaction of these two factors, planetary rotation and unstable stratification, can

equally result in generation of net helicity fluctuations of both signs - positive and negative - due to random ascending/descending flows initiated by thermal instability. Also, one should not expect distinctly non-zero total helicity generation by highly chaotic turbulent convection in the rotating atmosphere, however, could not exclude at all some spontaneous generation of its certain background value, e.g., due to fluctuated clustering of right-handed and left-handed elements on the scale compared with that of the computational domain.

It is worth noting in our discussion one more factor of helicity generation that was deliberately excluded from the initial statement of the problem in (M06). This is the vertical shear of horizontal wind (also, some shorter synonyms are often used for it, such as the vertical wind shear or simply, the vertical shear). It is observed widely in different atmospheric phenomena, and at the same time is well-known as an effective mechanism of helicity production, see, e.g., Lilly (1986); Davies-Jones et al. (1990); Weisman and Rotunno (2000), and references therein. In tropical meteorology, however, it is also well-known (Gray, 1975, 1979; Emanuel, 2003) that tropical cyclogenesis only occurs in environments characterized by small vertical wind shear (although one can observe intense shear flows in developed hurricanes). That is why, initial conditions in (M06) envisaged a favorable kinematic environment for genesis, i.e., zero ambient mean flow that implied the absence of vertical wind shear.

Both Coriolis force and buoyancy forces were prescribed by the governing equations of atmospheric hydro-thermodynamics within the RAMS model applied in (M06), meanwhile, in order to induce convective instability the initial conditions essentially contributed.

The numerical simulations in (M06) commenced with a favorable thermodynamic environment, i.e., a conditionally unstable troposphere overlying a warm ocean with sea surface temperature (SST)  $\geq 26^{\circ}\text{C}$ . This SST value is well known in tropical meteorology as one of a set of necessary conditions which are favorable for tropical cyclogenesis (Gray, 1975, 1979; Emanuel, 2003).

The initial temperature structure was the mean Atlantic hurricane season sounding (Jordan, 1958). This sounding was representative of non-Saharan-Air-Layer air (Dunion and Velden, 2004). With a SST of  $29^{\circ}\text{C}$  (Experiments A1, A2, B3, C1, C3, and E1 which are analyzed in the present paper, see Table 1) the soundings contained approximately  $997 \text{ J kg}^{-1}$  of 1-km mixed-layer CAPE based on pseudo-adiabatic ascent.

For the majority of the sensitivity experiments in (M06), the low- to mid-troposphere ( $z < 6 \text{ km}$ ) was moistened near the center of the initial MCV. The moisture enhancement was assumed to be the result of enhanced sea-to-air moisture fluxes in association with the weak MCV surface circulation. The moisture anomaly had a mixing ratio surplus of approximately  $1.3 \text{ g kg}^{-1}$  on  $z = 0$  near the MCV center. For the control experiment A1, the low-level moisture enhancement increased the 1-km mixed-layer CAPE to  $1526 \text{ J kg}^{-1}$  at the domain center. In Experiment B3 an opposite tendency was tested and low-level moisture was decreased by  $2 \text{ g kg}^{-1}$ .

One of the key players in many scenarios of tropical cyclogenesis is an initial mesoscale convective vortex (MCV) owning a vertical component of vorticity, which circulates cyclonically. The experiments in (M06) started with a MCV that was initially in hydrostatic and gradient wind balance. This enabled one to investigate in detail the convective/vorticity dynamics that ensued within this local environment using a near cloud resolving model. From the point of view of the vortex dynamo theory (Section 2.3), such MCV represents just that initial weak large-scale vortex disturbance or mean flow which is necessary for initiation of large-scale helical-vortex instability.

It is evident, that as soon as convection or an other vertical motion arises within the MCV circulation, it can act in concert with the MCV vertical vorticity and generate a vertical component of helicity.

To stir the convective instability ensuing from the initial thermal conditions, the so-called “warm bubble method” was applied in (M06). The warm bubble method represented an initial

local heating to create cumulus convection in the local environment of the MCV and might thus be regarded as a crude convective response for an elevated MCV subject to a brief episode of weak vertical shear.

In order to create a “warm bubble” (temperature surplus 2 K) at low levels ( $z = 2$  km), 50 km to the east of the MCV center, a local heating was applied for the first 300 s of numerical experiment. The resulting effects were quick to follow and well visible just after it, e.g. at  $t = 10$  min, that will be discussed in more detail in next sections. Such a standard expedient for stimulating convection was used in all numerical experiments of (M06), except Experiment B1, which was assigned to test an effect of the method on obtained results. The main results were found to be independent of the bubble initialization scheme.

It is important to examine what such couple of initial conditions – the warm bubble and cyclonic MCV – represents from the point of view of the “helical ideology”.

Local heating applied to create a warm bubble produced both vertical and horizontal temperature gradients in the environment. As it is well-known from the theory of thermal convection (Chandrasekhar, 1961; Gershuni and Zhukhovitsky, 1972), there exists a threshold vertical temperature gradient needed to initiate convection whilst the convective instability is unconditional under a horizontal temperature gradient, i.e., in the latter case a overturning convective circulation appears at any indefinitely small horizontal temperature difference. Such combination of instability factors makes theoretical investigation of the examined problem on convective stability quite complicated, moreover, with taking into consideration the fluid layer rotation. However, convective flows initiated by local heating from below in rotating fluid layers were studied in a number of laboratory experiments (e.g., Boubnov, 1997a,b; Bogatyrev et al., 2006, and references therein). They showed an existence of intense ascending plume flows localized just over the heated area and much broader and smoother overturning circulations which were gradually expanding for the whole experimental domain between the heater and colder periphery. The flows of both kinds interacted with each other generating strong enough horizontal and vertical components of vorticity.

When using the warm bubble method in a conditionally unstable troposphere, a similar combined situation of convective motions of two kinds was realized in (M06). This naturally resulted in generation of horizontal and vertical components of velocity and vorticity. As our current investigation shows (Section 5), their interaction produces a helicity field from the very first beginning of numerical experiment. Moreover, the generated helical field reveals a distinctly observed vertical contribution.

Results of (M06) demonstrated the metamorphosis from such initial mid-level cyclonic MCV to a tropical depression, which evolved further into a hurricane strength vortex, and highlighted the role of rotating cloud convection (vortical hot towers) in the observed process.

## 5. TC formation: helicity generation on cloud convection scales

In (M06) nineteen sensitivity experiments were carried out to thoroughly substantiate the proposed paradigm of tropical cyclogenesis. They were grouped into five categories: (A) horizontal resolution; (B) convective and thermodynamic processes; (C) perturbations in initial MCV structure; (D) absence of latent/sensible heat fluxes or momentum fluxes at ocean surface; and (E) absence of Coriolis parameter.

For our current purposes in helicity analysis we have chosen six experiments from different categories and presented them in Table 1.

Let us also remind about our given choice of the right-handed frame of reference (Cartesian and cylindrical ones are used in this study) as everything connected with helicity and discussed further is radically sensitive to it.

### 5.1. Experiment C1 “No Vortex”

It is quite interesting to discuss in detail a “helical” development in Expt. C1 (no initial MCV) during a few initial hours of simulation because it provides us with a unique possibility to follow a process of non-zero total helicity generation by convection for a simple enough, nearly a “template” convective episode in close to natural conditions of rotating moist and conditionally unstable troposphere layer in the Tropics. The process takes place in the absence of any introduced cyclonic circulation connected with MCV and without any imposed vertical shear of horizontal wind.

Our analysis of helical characteristics suggests examining full helicity density field (2) and its spatial contributions separately (3)-(6). Also mean total helicity (8), i.e. helicity density integrated over the computational domain and averaged by a number of grid points, together with its integrated spatial contributions (9) will be analyzed. In real atmospheric conditions there always exists a definite preferred direction due to gravity. It makes reasonable to introduce in our investigation vertical and horizontal helicity, the latter as a sum of two spatial horizontal contributions. In the subsequent discussion we will use terms “total helicity”, “horizontal helicity”, and “vertical helicity” for  $\langle H \rangle$ ,  $\langle H_{hor} \rangle$ , and  $\langle H_{ver} \rangle$ , correspondingly. As we could see in Section 3, non-zero total/horizontal helicity could be generated even when the vertical contribution of helicity vanished. However, that is only possible when the horizontal wind is changing with height, i.e. implies a vertical shear. **Thus, non-zero horizontal helicity can be considered as a sign of existing or emerging shear flow. Non-zero vertical helicity being a product of vertical velocity and vorticity can signal about vortical convection evolving in the examined area.**

Such an approach is also useful because of an accent made above on the special role of vertical flow component in both forcing simulation of helical-vortex flows by Levina (2006), L06 and cloud resolving atmospheric simulation for TC (M06). Bear this in mind, we will most be interested in those cases of non-zero total helicity generation when the vertical vortex flow is distinctly non-vanishing and contributes not certainly by its magnitude but by the linkage with horizontal counterparts.

Helical flow structure generated by the warm bubble can be well illustrated by Figure 5, where helicity field projections for Expt. C1 are shown after 10 (left column) and 140 minutes (right column) of simulation, respectively. Helicity data presented in Fig. 5 (a,c,e) were derived from the RAMS model output which was the first one with non-zero calculated fields available for our analysis (time increment for RAMS post-processing output was 10 min). The left column includes azimuthal averages of horizontal,  $HEL_{hor}$ , (a) and vertical,  $HEL_{ver}$ , (c) contributions of helicity density whilst their resultant field,  $HEL$ , is shown below (e). The pictures in the right column, Fig. 5 (b,d,f), show similar helicity fields at  $t = 140$  min, just at that time when the azimuthally averaged value of the vertical contribution of helicity density,  $HEL_{ver}$ , reached its maximal value over the whole experiment time of 72 hours.

As we can see (Fig. 5a,c,e), the vertical flow appears as a rotating updraft which generates small yet non-zero both the horizontal and vertical helicity. The former can be attributed to a weak shear profile generated by the the growing updraft which possesses horizontal velocity components due to its rotation whilst the latter is a contribution of vortical convection. For example, at height  $z = 1$  km its maximal relative vertical (planar) vorticity and vertical velocity are  $6.45 \times 10^{-6} \text{ s}^{-1}$  and  $1 \text{ m s}^{-1}$ , respectively (not shown). We found that a whole lifetime of the induced convective updraft was about 4 hours, including its intensification stage of approximately 140 minutes and degradation phase during next 100 minutes. At initial time horizontal contributions of helicity (Fig. 5a) were considerably larger than the vertical one (Fig. 5c) whilst the peak value of positive vertical helicity (Fig. 5d) at  $t = 140$  min was even slightly higher than the horizontal contributions.

The developing updraft intensified vigorously when ascending from low levels at  $z = 1-2$  km

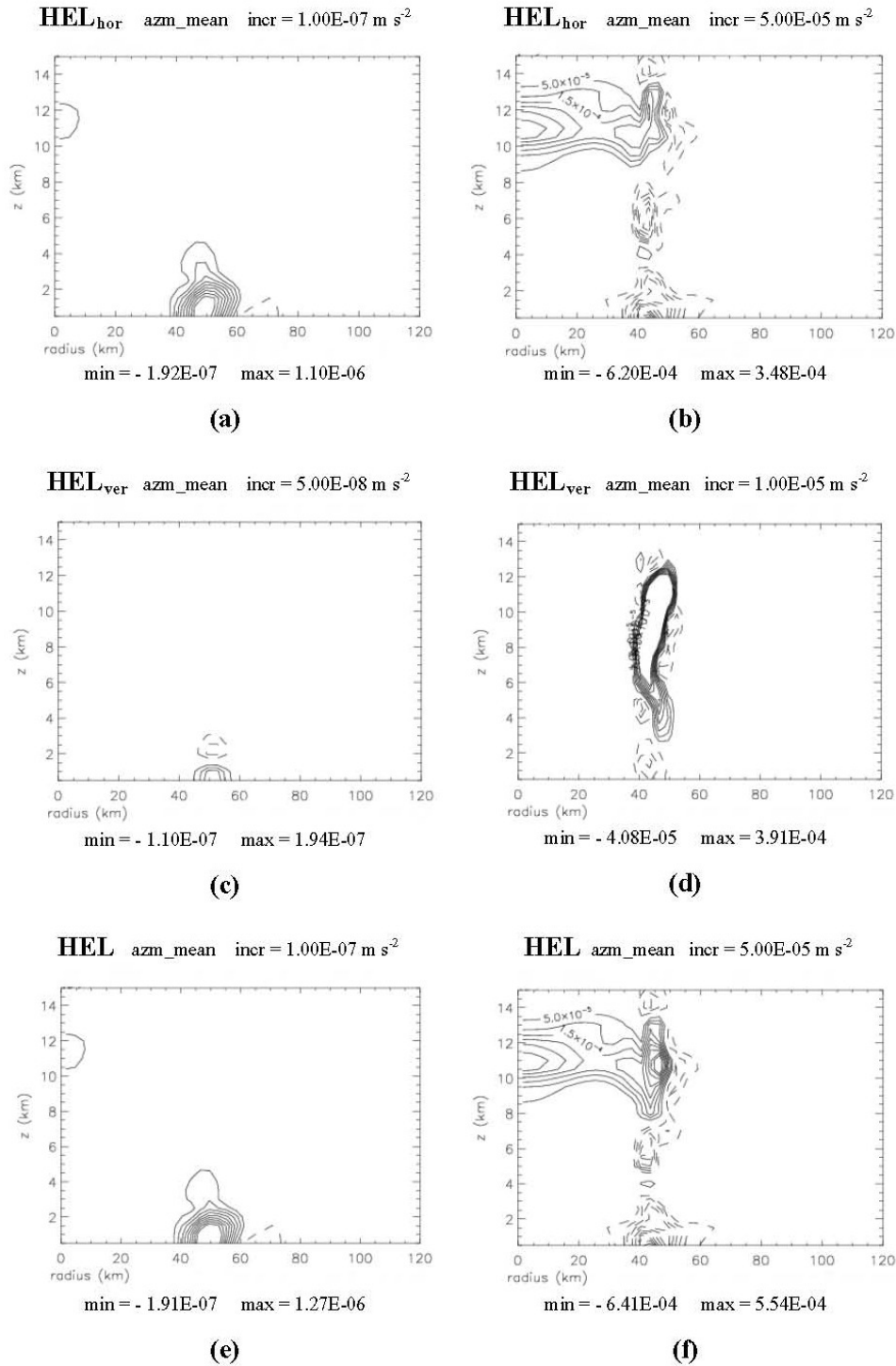


**Figure 5.** Helical flow structure generated by the warm bubble in Experiment C1 “No Vortex” at  $t = 10$  min (left column) and  $t = 140$  min (right column).

where its initial horizontal and vertical helicity was between  $-1.9 \times 10^{-7}$  and  $1.1 \times 10^{-6} \text{ m s}^{-2}$  (Fig. 5a), and  $-1 \times 10^{-7}$  and  $2 \times 10^{-7} \text{ m s}^{-2}$  (Fig. 5c), respectively. Dominated positive

vertical helicity at this time and during intensification stage can be explained by combination of dominated ascending flow and dominated cyclonic (positive) vertical vorticity due to planetary rotation in the given right-handed frame of reference. At the peak of its intensity the updraft reached the height  $z = 12\text{-}13$  km and possessed positive vertical helicity nearly  $4 \times 10^{-4} \text{ m s}^{-2}$  (Fig. 5d) which was 1000 times greater than that at  $t = 10$  min. Its maximal cyclonic relative vorticity and vertical velocity at  $t = 140$  min reached  $1.2 \times 10^{-3} \text{ s}^{-1}$  and  $2 \text{ m s}^{-1}$  ( $z = 1$  km). This vortical plume of about 10 km in diameter extended throughout the troposphere layer (Fig. 5d) and was warmer than the environment (not shown). Thus, in this convective episode we can identify a deep rotating helical updraft.

Horizontal contributions of helicity also increased and extended for a significant part of computational domain as we can see when comparing Figures 5a and 5b. However, such helicity field induced by the warm bubble alone was relatively weak and its vertical contribution (and, therefore, an area of possible linkage of horizontal and vertical vorticity lines) was localized only in close vicinity to the updraft.

Nevertheless, during the examined episode of deep convection, the distinctly non-zero (positive) total helicity,  $\langle H \rangle$ , was generated (Fig. 6a) since the very first beginning of the experiment. It reached the maximal value four hours after the vertical flow had its maximal intensity, and then, in the absence of updraft flow, was decreasing and became negative after  $t = 9$  h.

In our investigation the vertical contribution of total helicity,  $\langle H_{ver} \rangle$ , shown in Fig. 6c served us as a perfect marker of rotating convection evolution. Examination of vertical velocity and vorticity fields confirmed that they had their maximum/minimum values at the same time moments when the total vertical helicity was maximal/minimal (Fig. 6c). Anticipating our further discussion we can note that this contribution becomes zero nearly  $t = 4$  h and keeps vanishing during the rest of experimental time. This means an absence of noticeable rotating updrafts/downdrafts in the examined flow, i.e., the warm bubble alone has not been able to stir developing vortical deep convection in the examined space domain.

The analysis carried out for Expt. C1 brings a few useful insights:

- it gives a sample of rotating deep convective updraft which is easily generated in rotating conditionally unstable atmosphere,
- it demonstrates an intense and quick process of helicity field generation by a single convective updraft in a broad space area (Fig. 5b,d,f),
- it emphasizes two mechanisms of helicity generation, namely, by vertical shear that is responsible for the horizontal contributions of helicity, and vortical deep convection that brings the vertical helicity contribution,
- it points out that in vortical deep convection horizontal and vertical contributions of helicity can have very close magnitudes as, for example in Fig. 5b,d, their maximal values are  $3.48 \times 10^{-4} \text{ m s}^{-2}$  and  $3.91 \times 10^{-4} \text{ m s}^{-2}$ , respectively,
- it proposes the vertical contribution of helicity integrated over the computational domain and averaged by a number of grid points (Fig. 6c) as an appropriate tool to trace evolution of rotating updraft/downdraft flows,
- it shows non-zero total helicity generation by shear and thermal convection in rotating atmosphere.

However, such helical environment was found to be insufficient to initiate the large-scale helical instability as no TC formation was observed in Experiment C1. This allows suggesting that in addition to non-zero total helicity (which can be generated, Fig. 6a, even when the vertical contribution vanishes - Fig. 6c), a pronounced non-zero vertical contribution of helicity should exist providing the linkage of tangential wind (primary) and overturning (convective/secondary) circulation. One can easily reveal an “energetic” reason behind this since that is well-known that moist deep convection is an important supplier of energy into an incipient TC and should

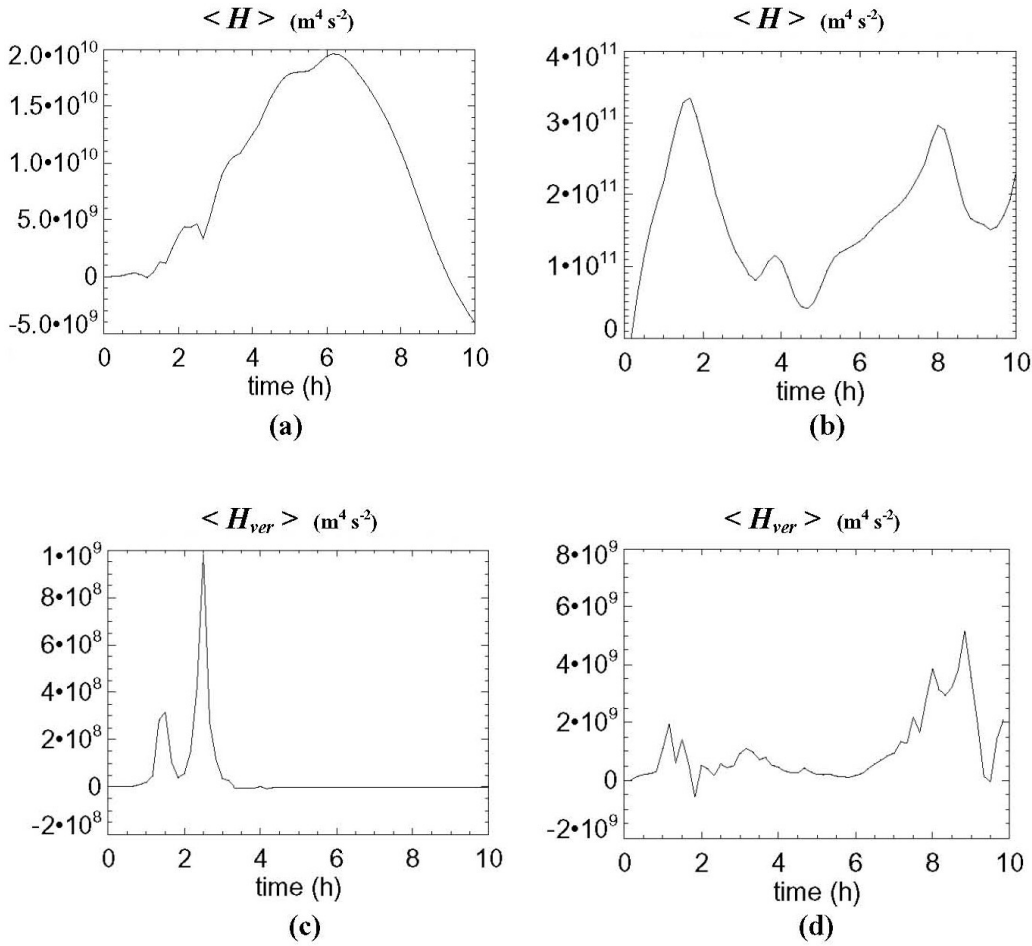


**Figure 6.** Total and vertical helicity evolution during initial 10 hours in Experiments C1 “No Vortex” (left column) and A2 “3 km” (right column).

play a crucial role in initiation of large-scale vortex instability.

### 5.2. A special note on importance of the vertical motion

At this juncture it is important to recall basic ideas of the theory of turbulence regarding a role of breaking the mirror symmetry in attempts aimed at achieving the dynamo effect. As it has been noted in (Moffatt, 1978), a lack of symmetry about planes perpendicular to the rotation vector  $\mathbf{\Omega}$  is necessary to provide the essential lack of reflectional symmetry in random motions that can lead to a large-scale helical instability. It was first pointed out by Steenbeck et al. (1966) that this lack of symmetry is present when buoyancy forces  $\rho\mathbf{g}$  (with  $\mathbf{g} \cdot \mathbf{\Omega} \neq 0$ ) act on fluid elements with density perturbation  $\rho'$  relative to the local undisturbed density  $\rho_0$ .

A thorough examination of the interaction between buoyancy and Coriolis force in generating helicity (the break of mirror symmetry) was carried out by Hide (1976, 1989, 2002). A number of equations were derived (when Coriolis acceleration was much less in magnitude than acceleration  $\mathbf{g}$  due to gravity) which were applicable to describe the flow energetics and allowed to interpret the observed processes of energy transformation. A special significance of the vertical component of the flow was emphasized (Hide, 2002) what is very important from the perspective of our current investigation. Despite this component is typically very small in comparison with

horizontal components, it plays a crucial role in conversion of potential energy associated with the action of gravity on density gradients into the kinetic energy of fluid motion. It is worth giving here a direct citation of (Hide, 2002): “Vertical motion is clearly linked with the helicity pseudoscalar, which in turn is linked with systematic variations of wind direction with height. Such variations provide weather forecasters with clues as to how atmospheric systems are likely to evolve”. Vertical motion will be under our close attention throughout the paper.

### 5.3. Experiment A2 “3km”– helicity generation in the presence of MCV

Let us start the subsection with a brief description of the initial mesoscale convective vortices, MCVs, applied in (M06).

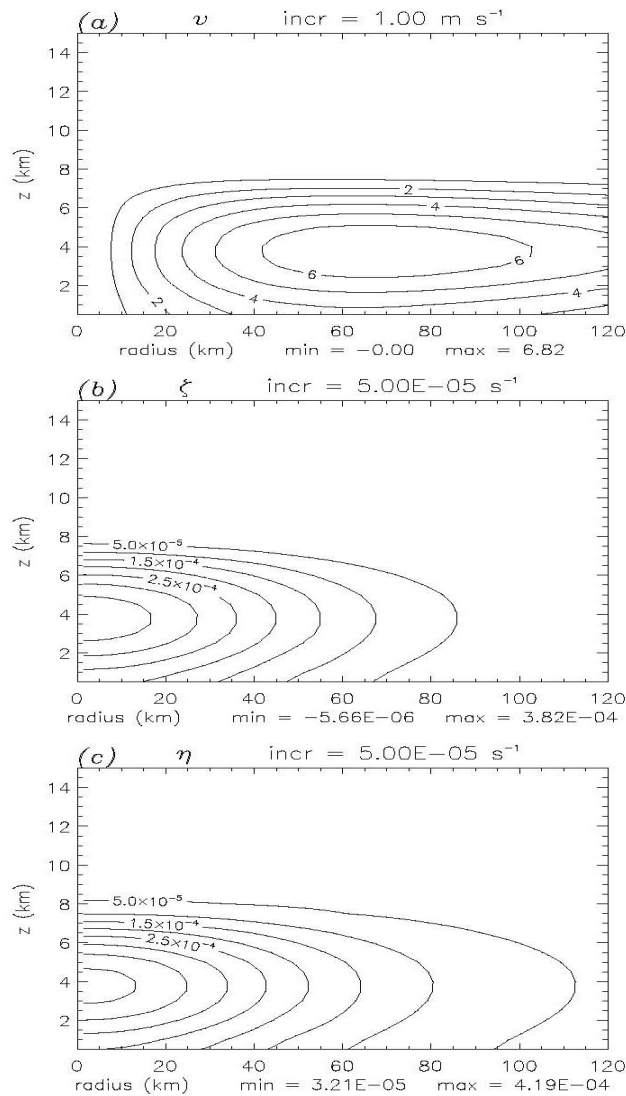


**Figure 7.** Initial MCV used for Experiment A2. Shown are azimuthal averages of (a) tangential wind, (b) relative vertical vorticity, (c) absolute vertical vorticity.

All initial MCVs used in idealized numerical experiments (M06) were cyclonic and, for simplicity, axisymmetric. Cyclonic vortices in the Northern Hemisphere, for which numerical

simulation in (M06) was carried out (the center of computational domain was located at latitude  $15^\circ\text{N}$ ), represented counterclockwise circulations and possessed positive vertical vorticity. They had their maximum vorticity near the  $z = 4 - 5$  km level, and their relative surface vorticity was of  $O(1 - 2 \times 10^{-4} \text{ s}^{-1})$ . Although the initial vorticity may, at first sight, seem large recall that a weak cyclonic circulation of only  $\sim 1 \text{ m s}^{-1}$  at radius of 20 km yields a surface relative vorticity of  $\sim 1 \times 10^{-4} \text{ s}^{-1}$ .

The bulk of the experiments in (M06) started with the MCV, which is shown in Figure 7, for example, as it was obtained under horizontal spatial resolution of 3 km applied in experiment A2. The vortex height and radius of maximum tangential wind (RMW) were 8 km and 75 km, respectively. It had a maximum tangential velocity of  $6.8 \text{ m s}^{-1}$  at a height of 4 km above sea level. The latitude at which the Coriolis parameter was calculated was taken to be  $15^\circ\text{N}$ . The mean vortex Rossby number  $R = v/fr$  associated with the initial MCV was  $\sim 2$  at the radius of maximum tangential wind.

It is quite another matter when such initial MCV enters into play. A set of pictures in Figure 8 demonstrates for Experiment A2 how a much more complicated and intense helicity field forms via interaction of the MCV and horizontal and vertical flow components produced by the warm bubble during a few initial hours.

If we compare Figures 5(a,c,e) and 8(a,c,e), which give helicity fields for Expt. C1 and A2, respectively, at the same starting time  $t = 10$  min, we can find corresponding typical values of about two orders of magnitudes higher under action of MCV in Expt. A2. In this case non-zero helicity is distributed over a wider domain what means that much more vortex lines can be linked and contribute to helicity generation.

In Expt. A2 rotating convective updraft is progressing much faster than that in Expt. C1 and reaches its peak of intensity in 70 min. At this time it extends throughout the troposphere up to  $z = 14$  km (Fig. 8d). In order to compare two cases we can give a typical value of positive vertical helicity  $\approx 10^{-3} \text{ m s}^{-2}$  (Fig. 8d), and similarly as in Expt. C1, for maximal vertical velocity  $3.2 \text{ m s}^{-1}$  and cyclonic relative vorticity  $1.7 \times 10^{-3} \text{ s}^{-1}$  (at  $z = 1\text{km}$ , not shown). These estimates are distinctly higher than those ones in Expt. C1 and have been attained two times faster.

However, the most striking speciality of the updraft in Expt. A2 is connected with its dipole structure, which is an interesting result originated from a very process of its formation. In Expt. C1 in the absence of MCV, an environment was not rich in horizontal and vertical vorticity. Vorticity was only generated by the rising bubble itself and intensified by stretching. This resulted in a considerably smaller intensity of Expt. C1 updraft. In Expt. A2 the process of rotating updraft formation and intensification occurs in the MCV environment, which is rich in vorticity, and is accomplished by tilting of horizontal vorticity and stretching of vertical vorticity, i.e. similarly to that described in detail for vortical hot towers and perfectly illustrated in Fig. 10 of (M06). A weak vertical shear profile of initial MCV (Fig. 7) generates radial vorticity of different signs below and upper  $z = 4$  km. The updraft induced overturning circulation also contributes to generation of horizontal components of vorticity. The developing updraft tilts radial vortex filament upward, generating a vertical vorticity dipole with negative relative vorticity radially inward (outward) at heights below (above)  $z = 4$  km while at the same time stretching MCV-generated vertical vorticity. As the updraft intensifies and deepens into mid and upper troposphere, both ambient and tilting-generated vertical vorticity is stretched even more.

The above described mechanism (M06) of horizontal vorticity transformation into the vertical one by a developing convective updraft can also be interpreted as an effective way for generation of the linkage of vortex lines of horizontal and vertical components of vorticity, i.e. helicity generation.

Thus, we can consider the updraft (Fig. 8d) as the first hot tower in the experiment A2.

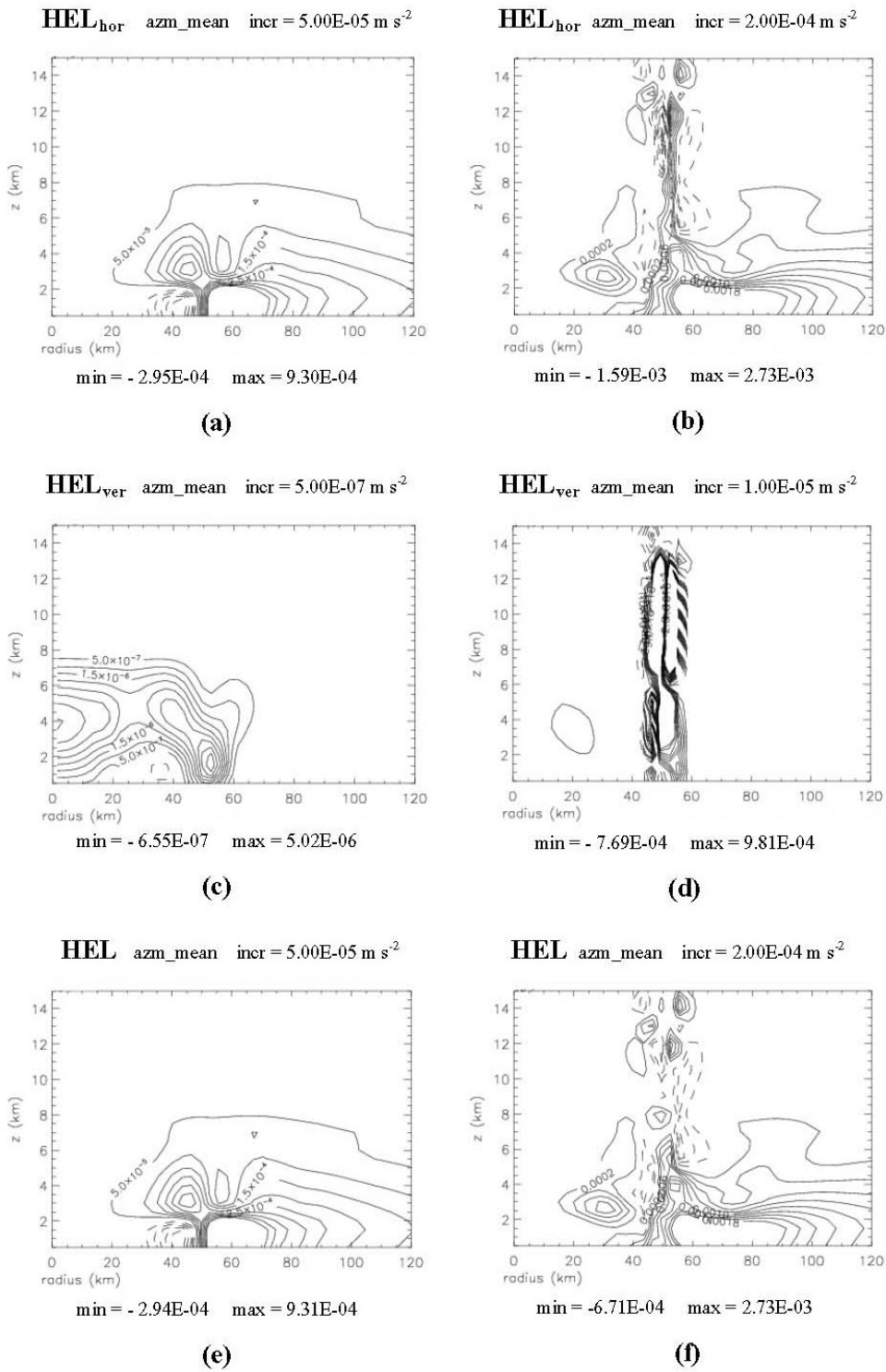


**Figure 8.** Helical flow structure generated by interaction of the warm bubble and initial MCV in Experiment A2 at  $t = 10$  min (left column) and  $t = 70$  min (right column).

This VHT is very similar to a VHT which was described in detail in (M06) as the first one obtained in Expt. A1 (2 km horizontal space resolution) within the very first hour of simulation and shown in Fig. 9 (M06). The first VHT in Expt. A2 is an essentially helical flow and found to be strong enough to contribute to the system scale dynamics by generation transient yet well visible signs of the transverse overturning circulation – averaged radial and vertical flows. Azimuthally averaged fields for this case at  $t = 70$  min corresponded to the maximal VHT intensity are shown in Fig. 9. This highlights the VHT role as a link between the initial system-scale tangential circulation created by the MCV (primary circulation) and a newly emerging large-scale overturning circulation (secondary circulation).

A peak value of the vertical helicity,  $\langle H_{ver} \rangle$ , corresponded to the first VHT is  $1.9 \times 10^9 \text{ m}^4 \text{ s}^{-2}$  (Fig. 6d), which is 2 times higher than for the updraft in Expt. C1 (Fig. 6c). The maximum of total helicity,  $\langle H \rangle$ , (Fig. 6b) generated within the initial time span in Expt. A2 is about  $3.3 \times 10^{11} \text{ m}^4 \text{ s}^{-2}$ , which is more than 10 times greater than in the previous case (Fig. 6a).

The obtained distribution of total helicity is characterized by an increased contribution of the vertical flow component and gives the degree of linkage of the vortex lines of horizontal and vertical vorticity, which is found to be sufficient to generate large-scale vortex instability. It is important to point out that such linkage of vortex lines is generated by the first VHT which is a representative of rotating deep convection.

#### 5.4. A practical advantage of total helicity calculation

Analysis carried out for helicity generation during a few initial hours in Expts. A2 and C1 showed in detail how this process can be developing in natural conditions of the Earth’s tropical atmosphere. A special role of vortical moist convection was emphasized. It was demonstrated that rotating convective structures of two kinds were the main contributors to generation and amplification of vorticity field with the linkage of vortex lines of flow components. These two kinds of convective structures emerged in dependence on the initial environmental conditions in a form of rotating helical updrafts or rotating helical dipole structures - Vortical Hot Towers (VHTs). The main difference originated from whether vorticity-rich environment was prepared by the initial MCV (Expt. A2) or not (Expt. C1).

For our further analysis it is useful to give in Table 2 the highest values of total helicity,  $\langle H \rangle$ , attained due to the initial conditions. As we can see, in Experiment C1 “No Vortex” it is in order of magnitude lower than in four other experiments. Just this experiment in (M06) did not reveal any signs of large-scale vortex instability whilst in Experiments A2, B3, C3, and E1 a metamorphosis was successful to surface-concentrated warm core tropical depressions although characterized of quite different strength of tangential circulation.

At this point we may hypothesise that the initial break of mirror symmetry in Experiment C1 was not strong enough to initiate the large-scale instability.

Total helicity describes a special structure of vortex velocity field characterized by the linkage of vortex lines. In our case, the vortex field is essentially three-dimensional due to developed thermal convection. Different conditions and physical mechanisms contribute to generate such helical structure of vortex velocity field, and helicity can be chosen as a quantitative mathematical measure to describe the resulting effects of their interaction. In tropical cyclone investigations a practical advantage may be gained by using helicity in order to give quantitative prediction for large-scale vortex instability. Based on the above results for the problem formulation as posed in (M06), we may suggest that different effects contributing to initial conditions should provide total helicity of about  $2.0 \times 10^{11} \text{ m}^4 \text{ s}^{-2}$  and higher in order an upscale organization of moist convective atmospheric turbulence becomes possible.

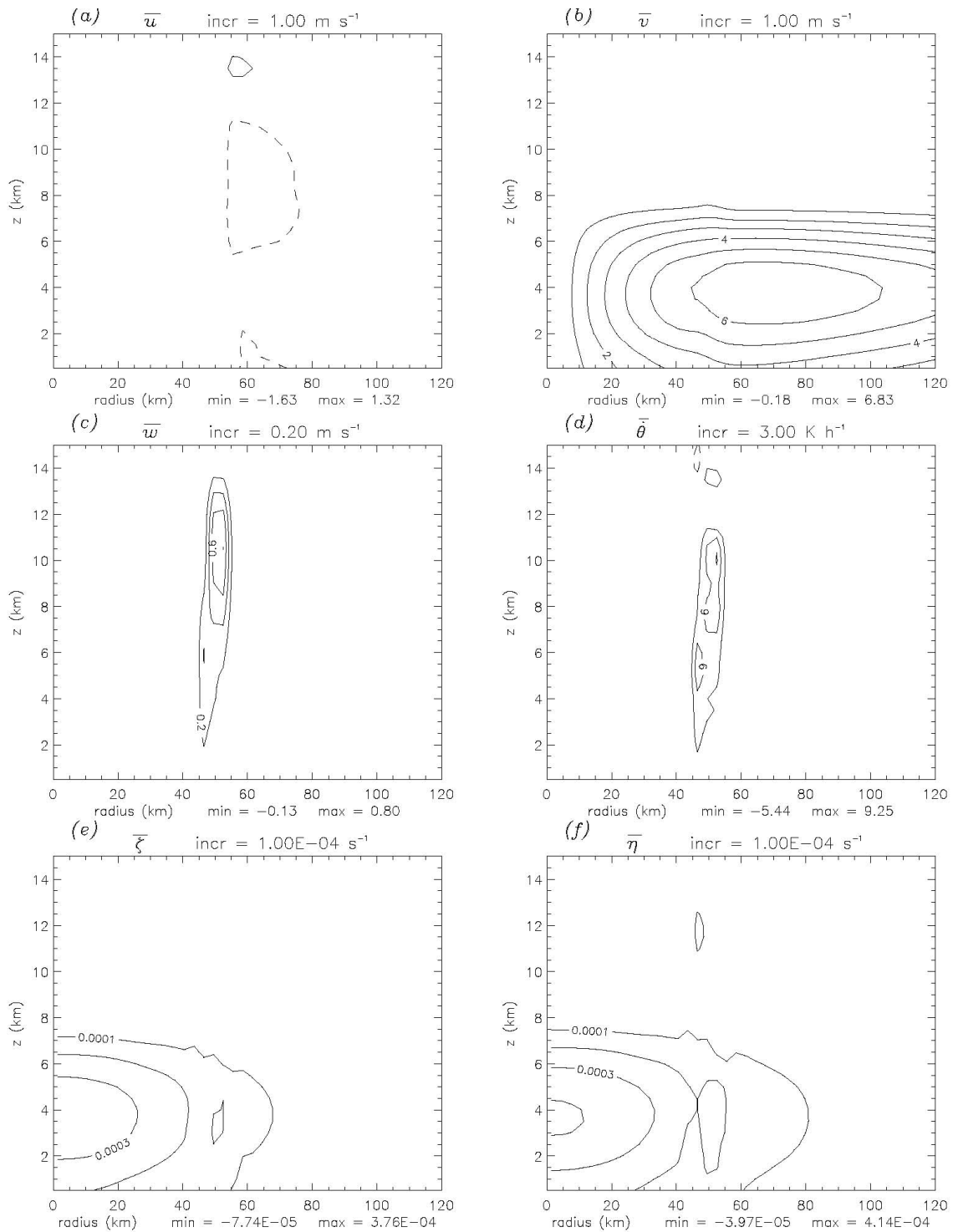


**Figure 9.** Azimuthal averages of (a) radial wind, (b) tangential wind, (c) vertical velocity, (d) diabatic heating rate, (e) relative vertical vorticity, and (f) absolute vertical vorticity at  $t = 70$  min from Experiment A2. The zero contour is omitted. Negative contours are dashed.

## 6. TC formation: pinpointing key events – TC genesis, tropical depression (TD) formation, TC intensification stage

In this work we have no ambition to discover and propose a new mechanism for TC formation which is based on helicity generation. This is simply because helicity generation is not a new physical process yet a result of variety of other effects acting in the tropical atmosphere.

However, analysis of helicity may bring a new insight into atmospheric phenomena that lead to tropical cyclone development. It will be demonstrated further that based on helicity role in tropical cyclone genesis and intensification, important quantitative measures may be given to trace the large-scale vortex instability evolution, namely:

- to identify safely the fact of tropical cyclone genesis as an emergence of energy-self-sustaining helical vortex,
- to distinguish as different events TC genesis and TD formation,
- to try discerning TC genesis and intensification stages based on what is a leading mechanism contributing to helicity generation.

### 6.1. Quantitative analysis for evolution of large-scale vortex instability

At this juncture it is useful to follow paper (Montgomery & Smith, 2011) and remind about the macro (non-turbulent) motions within a tropical cyclone vortex. In terms of the macro variables, the tropical cyclone consists of a horizontal quasi-axisymmetric circulation on which is superposed a thermally-direct transverse (overturning) circulation. These are sometimes referred to as the “primary” and “secondary” circulations, respectively (see, e.g., Fig. 3). The former refers to the tangential or swirling flow rotating about the central axis, and the latter to the transverse or “in-up-and-out circulation” (low and middle level inflow, upper-level outflow, respectively). When these two components are combined, a picture emerges in which air parcels spiral inwards, upwards and outwards. The combined spiralling circulation is called energetically direct because the rising branch of the secondary circulation near the center is warmer than the subsiding branch, which occurs at large radial distances (radii of a few hundred kilometers). When warm air rises (or cold air sinks), potential energy is released (Holton 2004, p339).

In the majority of numerical experiments (M06), a weak tangential circulation existed in low and mid troposphere (with a maximal wind at  $z = 4\text{--}5$  km) from the very first beginning due to the initial MCV. The secondary circulation in cases (M06) examined in the present work appeared after several hours of flow development as a result of self-organization of vortical cloud convection or did not appear at all in unfavorable environment (Expt. C1, no initial MCV). The time interval needed for the secondary circulation to emerge depended on initial conditions.

For purposes of quantitative analysis in addition to helical characteristics we will be examining kinetic energies of primary and secondary circulations calculated similarly to formulae (11) as squares of corresponding components of velocity in the cylindrical coordinates, integrated over the computational domain and normalized by number of grid points. Thus,  $\langle E^P \rangle$  characterizes the intensity of primary tangential circulation whilst  $\langle E^S \rangle$  concerns the secondary circulation formed by the radial and vertical components of velocity. It should be noted that unlike initially organized tangential circulation, radial and vertical flows contributing to the secondary circulation are chaotic and weak enough during an initial time span. Nevertheless, it results in a small non-zero kinetic energy,  $\langle E^S \rangle \neq 0$ . In order to diagnose an emerging secondary circulation, azimuthally mean fields of radial and vertical flow components will be analyzed.

We will further apply our approach to examine and compare TC development in five experiments A2, B3, C1, C3 and E1, all of which were simulated by using the identical 3 km horizontal grid increment. Let us start with a comprehensive discussion of Experiment A2 “3km” that demonstrates a whole evolution of tropical cyclone, including both genesis and

intensification stages, up to hurricane strength.

*6.1.1. Diagnosing of TC genesis – when the vortex becomes energy-self-sustaining* In this section and the next one, we are going to trace the hurricane vortex development and pinpoint by quantitative criteria two milestones in its evolution, namely, TC genesis and TD formation. To this purpose we will use kinetic energy and helicity characteristics (Fig. 10) as well as a set of other data gained from snapshots of spatial velocity, vorticity, helicity and temperature fields at horizontal and vertical cross-sections.

The Expt. A2 started with kinetic energy of the primary tangential circulation,  $\langle E^P \rangle$ , equal to  $0.45 \times 10^{16} \text{ m}^5 \text{ s}^{-2}$  (Fig. 10), entirely generated by the initial MCV, which had the maximum tangential wind  $6.8 \text{ m s}^{-1}$  at  $r = 75 \text{ km}$  and  $z = 4 \text{ km}$ . Initially, the secondary transverse circulation was absent that implied vanishing kinetic energy,  $\langle E^S \rangle = 0$ . The maximal value of total helicity,  $\langle H \rangle$ , generated by the initial conditions in this experiment was  $3.3 \times 10^{11} \text{ m}^4 \text{ s}^{-2}$  (Table 2). This is an order of magnitude higher than  $2.0 \times 10^{10} \text{ m}^4 \text{ s}^{-2}$ , which was insufficient for initiating the upscale organization in Expt. C1 (section 5).

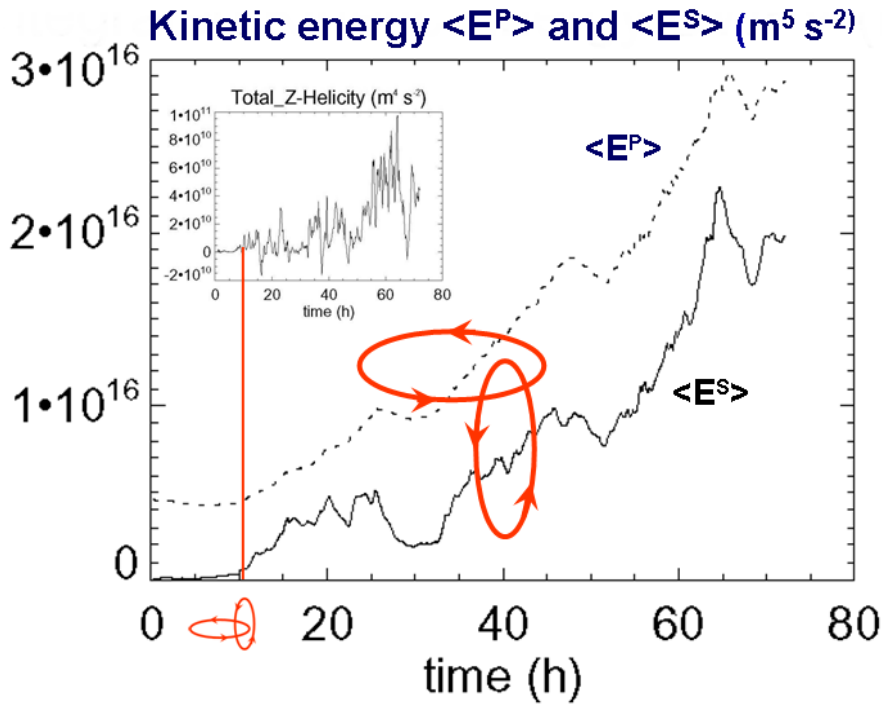


**Figure 10.** TC genesis at  $t \sim 10 \text{ h}$  – the linkage of the primary and secondary circulation makes the forming vortex an integral helical system which is energy-self-sustaining due to the “helical” feedback between the circulations.

During the first 10 hours, the tangential circulation is slightly weakening against its initial energy value (Fig. 10) and the maximal tangential wind undergoes a decrease from  $6.8 \text{ m s}^{-1}$  to  $6.0 \text{ m s}^{-1}$ , whilst  $\langle E^S \rangle$  becomes slowly increasing near  $t = 5 \text{ h}$ . One can interpret the latter as a sign of developing thermal convection. Our examination of the vertical velocity and vorticity fields confirmed a weak thermoconvective activity with no strong rotating updrafts at that time.

A few rotating convective flows become visible (with maximal vertical velocity about  $2.5 \text{ m s}^{-1}$  and cyclonic vertical relative vorticity  $3.0 \times 10^{-3} \text{ s}^{-1}$  at  $z = 1 \text{ km}$ ) at  $t = 6 \text{ h}$ . Near this

time a process of merging of convective cells starts. This phenomenon was described in detail, analyzed quantitatively and interpreted in (M06) as a manifestation of upscale organization of atmospheric rotating moist convection. As it was shown in (M06,LM10,LM11), the process of merging is accompanied by not only an emergence of larger and stronger convective structures but also an increase in the background vorticity and helicity in adjacent areas. Convective activity is progressing quickly during  $t = 6-9$  h and such burst of vortical convection is well seen in the vertical and total helicity evolution (Figs. 6b,d; 10). This marks an emergence of a whole population of convective updrafts, which interact with each other by merging, and result in more intense structures. Between them, there appear a few ones, which represent cyclonically rotating deep convection - vortical hot towers (VHTs) of different horizontal and vertical sizes and intensity (the maximal vertical velocity and vorticity during these few hours are increasing up to  $3.5 \text{ m s}^{-1}$  and  $5.0 \times 10^{-3} \text{ s}^{-1}$ , correspondingly, at  $z = 1 \text{ km}$ ). Within this time interval the most intense updrafts have 5–10 km in diameter and are gradually with time growing in height from 4–6 km up to 8–10 km.

Emerging and intensifying rotating convective flows generate a non-vanishing and increasing third (vertical) contribution of helicity (Fig. 10, upper panel) and, thereby, a local linkage of vortex lines of horizontal and vertical flow components in a vicinity of each rotating updraft.

An uniqueness of such rotating convective flow (updraft/VHT) consists in its “dual” nature comprising elements of both the primary and secondary circulation. Each rotating convective structure contributes simultaneously to both the tangential horizontal and convective vertical circulation, namely, by its vertical vorticity to the former and by its vertical motion to the latter. Moreover, so long as a vicinity of each updraft is overheated against the environment due to sensible or latent heat release (Fig. 9d), such ascending flow creates horizontal temperature gradients thereby producing a local overturning circulation. The newly created local overturning circulation includes a weak shear profile, and the whole local configuration can contribute to the main mechanism of vertical vorticity (and helicity) generation discussed in previous sections. Thus, the rotating convective structure represents a natural link between the tangential and transverse circulation on its local scale whilst, as we expect, their developed population of strong enough intensity should tightly link the primary tangential and the secondary transverse circulation on the system scale.

**To measure a degree of such linkage is just the main function of the quantity introduced above and as known as “helicity”.**

The locally generated linkage of the vortex lines results in a mutual intensification of tangential and vertical flow components and contributes to integral flow characteristics. This is well pronounced in evolution of helical characteristics (Figs. 6b,d), which are quite sensitive to such changes. An emerging vertical helicity generated by developing rotating convection near  $t = 6$  h immediately leads to a significant increase in horizontal contributions of helicity and, consequently, in total helicity. Thus, in our case under consideration (Fig. 6d), an increase in the vertical contribution of helicity from zero up to approximately  $5.0 \times 10^9 \text{ m}^4 \text{ s}^{-2}$  within 6–9 h results in an amplification of horizontal/total helicity from  $1.5 \times 10^{11} \text{ m}^4 \text{ s}^{-2}$  up to  $3.0 \times 10^{11} \text{ m}^4 \text{ s}^{-2}$  (Fig. 6b). Just at this time,  $t = 6$  h, a slight yet distinct increase in the kinetic energy  $\langle E^S \rangle$  starts due to both increased vertical and radial flow components.

Near  $t = 10$  h dramatic changes in the flow intensity attract our attention – kinetic energy of the transverse circulation,  $\langle E^S \rangle$ , increases sharply and soon after this, kinetic energy of the tangential circulation,  $\langle E^P \rangle$ , becomes increasing as well (Fig. 10). This emerging mutual intensification of both circulations marks a critical point in a process of TC formation when **the vortex becomes energy-self-sustaining**. Exactly this time moment in TC evolution may be considered as an event of tropical cyclone genesis.

In order to identify reasons which are behind the observed phenomenon, let us search for explanations in corresponding flow structure and dynamics. Indeed, an intense helical updraft–

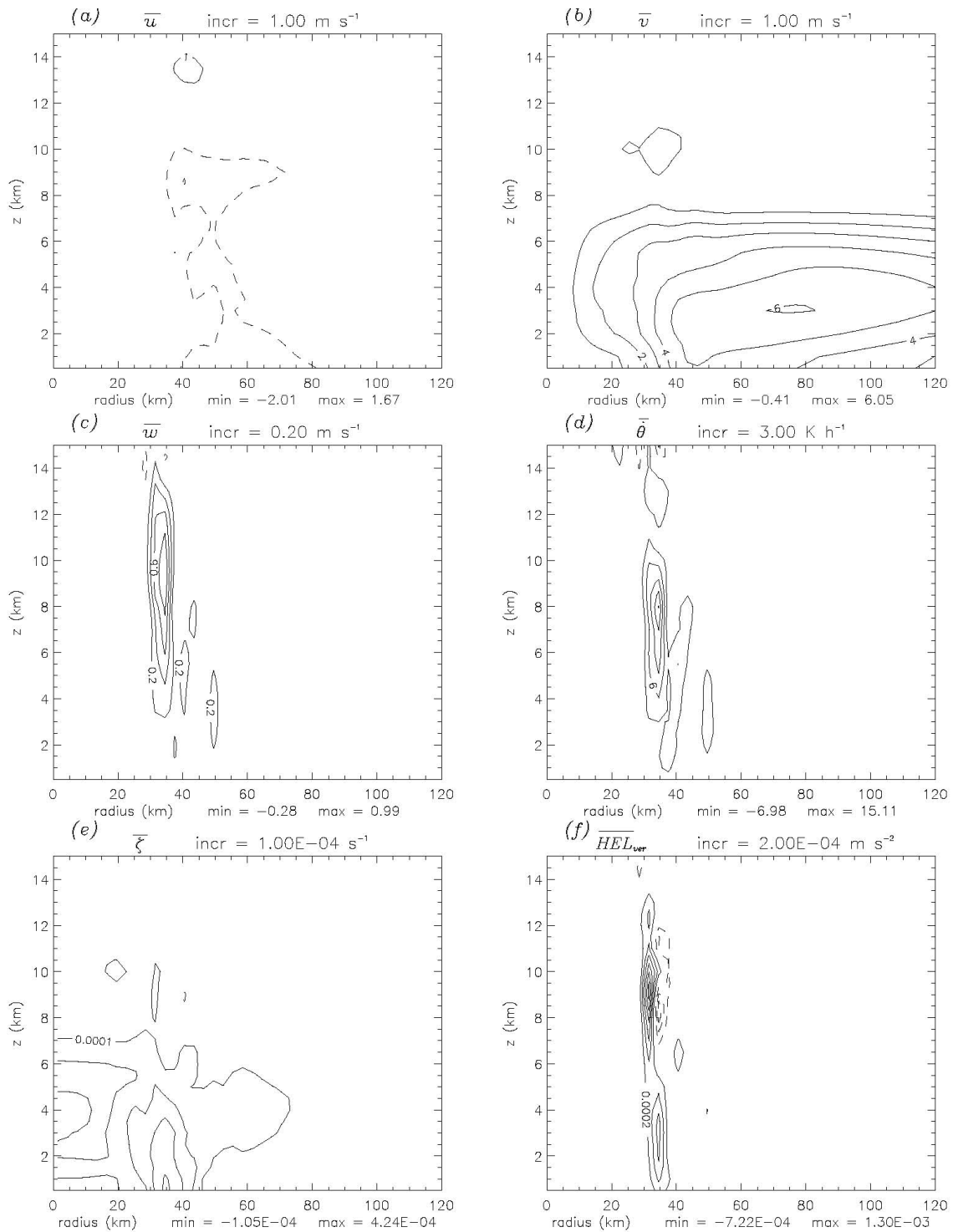


**Figure 11.** Azimuthal averages of (a) radial wind, (b) tangential wind, (c) vertical velocity, (d) diabatic heating rate, (e) relative vertical vorticity, and (f) vertical contribution of helicity at  $t = 10$  h from Experiment A2. The zero contour is omitted. Negative contours are dashed.

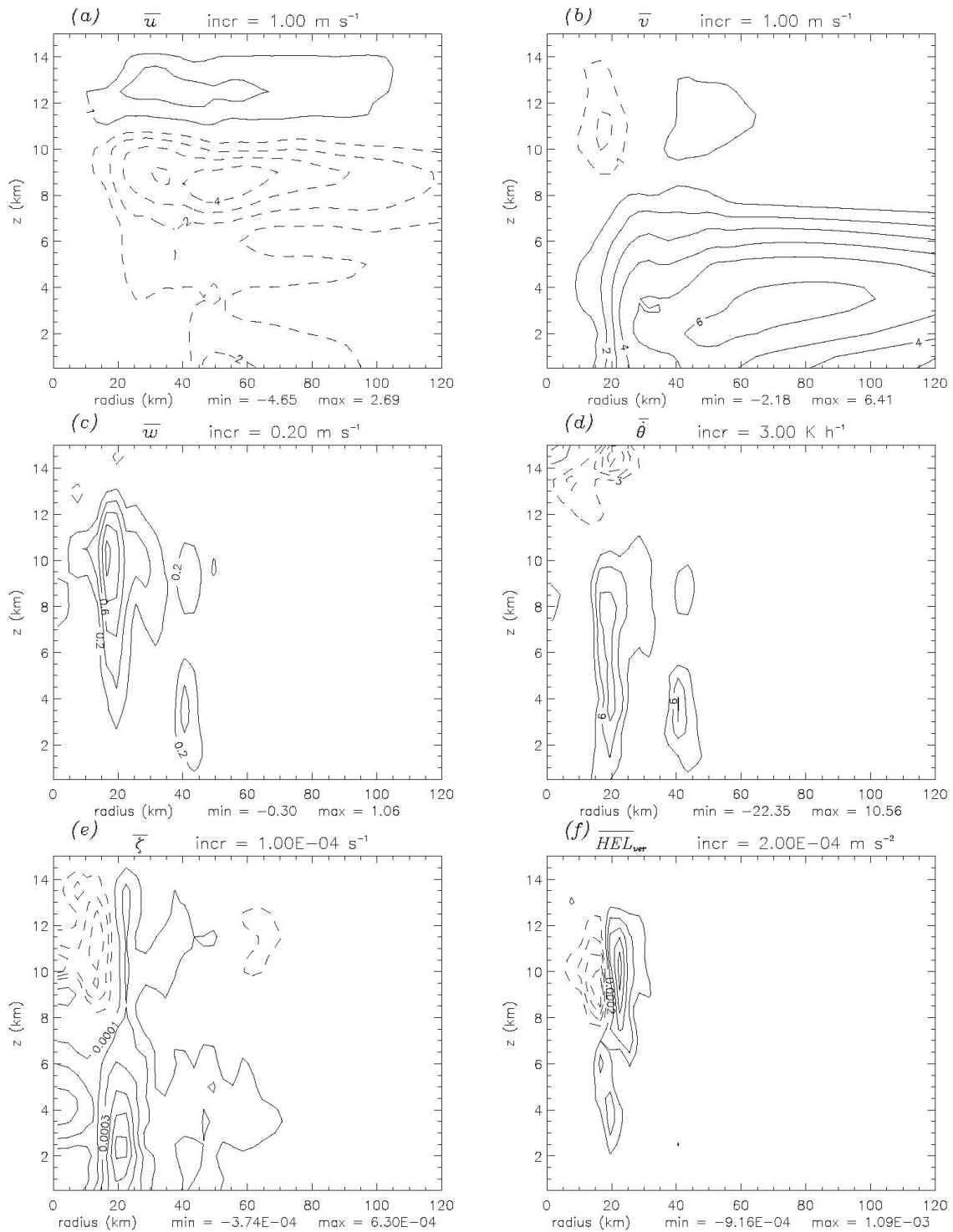


**Figure 12.** Azimuthal averages of (a) radial wind, (b) tangential wind, (c) vertical velocity, (d) diabatic heating rate, (e) relative vertical vorticity, and (f) vertical contribution of helicity at  $t = 12$  h from Experiment A2. The zero contour is omitted. Negative contours are dashed.

VHT of about 14 km in height appears just at that time,  $t = 10$  h (Fig. 11c,d,f). The VHT is found to be strong enough to not only generate a large (tens of kilometers in horizontal directions and throughout the whole troposphere layer up to 14 km in height – Fig. 11a,c) transverse circulation for a short instance as it was at the initial stage (section 5.1.2, Fig. 8) but for giving start to the formation of stable system-scale (hundreds of kilometers horizontally) secondary circulation during  $t = 10$ –12 h. In Fig. 12 plotted for  $t = 12$  h, one can see the already formed transverse circulation with a pronounced low and middle level inflow, developed rising flow and upper level outflow. The circulation is sustained and linked with the primary circulation by the intense VHT and a whole family of smaller and less intense rotating convective flows.

During development of such flow configuration, vertical and total helicity are increasing and reach their values  $1.5 \times 10^{10} \text{ m}^4 \text{ s}^{-2}$  and  $4.0 \times 10^{11} \text{ m}^4 \text{ s}^{-2}$ , respectively, at  $t = 12$  h that are about two times greater than those at  $t = 10$  h. This considerable increase in helicity values marks a qualitative change in a large-scale flow structure when the linkage of the system-scale tangential and transverse circulation emerges. **This means that the forming large-scale vortex becomes an integral helical system.** This is only possible due to significant growth of number of rotating convective structures which are much more intense than those at earlier times.

Since this point one can observe consequently increasing intensity of both the primary and secondary circulation with time, yet, interrupted periodically ( $\sim 24$  h) due to diurnal cycle.

The tendency is perfectly seen in kinetic energy evolution (Fig. 10). This indicates that a positive feedback has formed between the circulations and resulted in a developing large-scale vortex instability. The feedback is sustained by energy of vigorous vortical convection (see, the vertical helicity evolution in Fig. 10), which is gradually intensifying with time. The existence of such intense rising warm flows suggests a release of potential energy that is converted into kinetic energy of developing large-scale helical vortex. The active feedback provides energy exchange between the primary and secondary circulation and their further mutual intensification.

Progressing instability develops as multiple diabatic vortex mergers due to convergence initiated by the strengthening transverse circulation alongside the more familiar dry adiabatic vortex merger of convectively generated remnants.

*6.1.2. Diagnosing of TD formation* Simultaneously with formation of the secondary circulation during  $t = 10$ –12 h that reveals itself in emergence and further increasing intensity of near surface and middle level radial inflow and upper-level outflow (Figs. 11a, 12a) as well as in intensification of vertical motion (Figs. 11c, 12c), we can observe when comparing Figs. 11(b) and 12(b), how the maximum of tangential wind starts shifting from middle levels to the surface and its slight growth within these two hours, from  $6.0$  to  $6.4 \text{ m s}^{-1}$ . The tendency is persisting during next 5-6 hours and accompanied by generation of a cold descending cyclonic flow and a lower branch of radial outflow near the center of domain. The flows are first extending along the height at middle levels from  $z = 4$ –5 km up to  $z = 9$  km (not shown). An emergence of such flows leads to decreasing total helicity (Fig. 13a) after  $t = 14$  h and culminates in its negative value  $\langle H \rangle = -4.0 \times 10^{11} \text{ m}^4 \text{ s}^{-2}$  near  $t \approx 16.5$  h, which is found to be the biggest negative value of total helicity during the whole experiment A2. It should be pointed out that total helicity becomes negative only once in Expt. A2, for these two hours, 16–18 h. Within the same time span the vertical helicity is also negative and confirms the possible existence of descending cyclonic flow. This quantity has its maximal local negative value  $\langle H_{ver} \rangle = -1.6 \times 10^{10} \text{ m}^4 \text{ s}^{-2}$ , near the same time as total helicity, namely at  $t \approx 16.5$  h – Fig. 13b.

The corresponding flow structure at  $t = 16.5$  h is given in Fig. 14. As we can see, at this time the lower radial outflow, Fig. 14a, occupies a central area up to 20 km along the radius and along the height deepens from mid levels (6–7 km) up to the surface, 0–0.5 km. This is also an

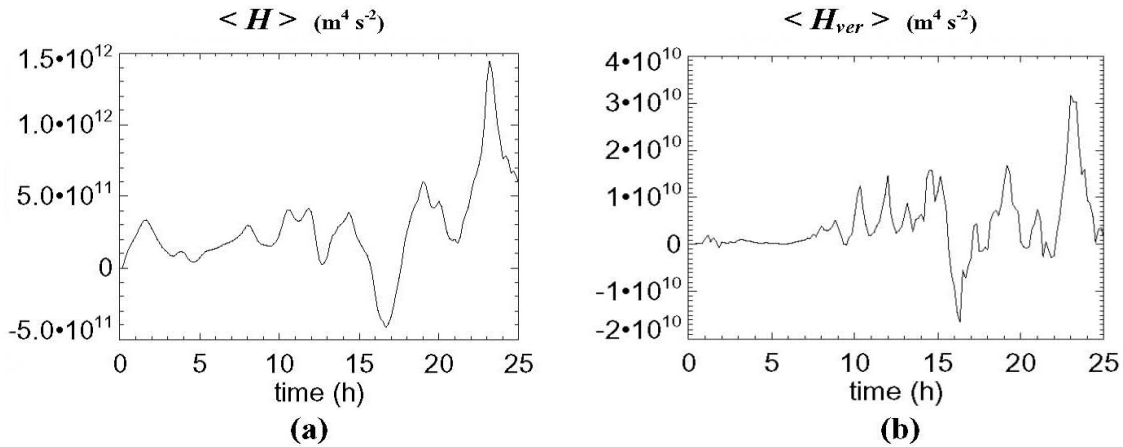


**Figure 13.** Total (a) and vertical (b) helicity evolution during initial 25 hours in Experiment A2 “3 km”.

area of cold (d) cyclonic (e) downdraft flow (c) with a maximum mean speed of sinking about  $1.2 \text{ m s}^{-1}$ .

However, the most impressive result of the observed flow evolution is pronouncedly seen in Fig. 14b,d,e where one can find a newly formed surface-concentrated warm-core vortex on the atmospheric mesoscale. The vortex can be identified as a tropical depression (TD) characterized by the maximal near-surface tangential wind of  $9.3 \text{ m s}^{-1}$  at radius  $r \sim 30 \text{ km}$ . The kinetic energies of the primary and secondary circulations in the formed TD are about  $0.6 \times 10^{16} \text{ m}^5 \text{ s}^{-2}$  and  $0.35 \times 10^{16} \text{ m}^5 \text{ s}^{-2}$ , correspondingly – Fig. 10.

During 16.5–18 h the flow structure in the central area is gradually restoring so that at  $t = 18 \text{ h}$ , the lower radial outflow and cold cyclonic flow are found to be at middle levels again – Fig. 15a,c,d. The TD vortex undergoes a slight decrease of maximum near-surface wind speed up to approximately  $8.8 \text{ m s}^{-1}$  – Fig. 15b. Such flow rearrangement is accompanied by changing total helicity (Fig. 13a) that reaches zero just at that time  $t = 18 \text{ h}$ .

It should be particularly noted that after  $t = 18 \text{ h}$  the total helicity becomes only positive and persistently increasing for the remainder of experiment. Thus, the negative total helicity describes a flow configuration that corresponds to the process of TD formation. The intrinsic features of such configuration are the surface-concentrated warm-core mesoscale TD vortex, the lower branch of radial outflow and cold descending cyclonic flow, both of which extended from the surface to middle levels near the center of domain. These findings can be useful for TD diagnosing by means of numerical atmospheric modeling systems.

The newly formed TD vortex is energy-self-sustaining and intensifying as the kinetic energy evolution shows in Fig. 10. This is only possible due to the system scale linkage of the primary and secondary circulations.

*6.1.3. Preliminary ideas about helicity advantage to diagnose TC intensification stage* We would also try and interpret further evolution of the TD vortex based on the same numerical data gained from (M06). However, as it is evident, in the intensifying tropical cyclone a role of helicity generation at lower levels due to developing near surface vertical shear and via interaction with the boundary layer should increase dramatically. Because of this, four horizontal levels within lower 0–2 km used in numerical experiments (M06) could bring only preliminary estimations and conclusions.

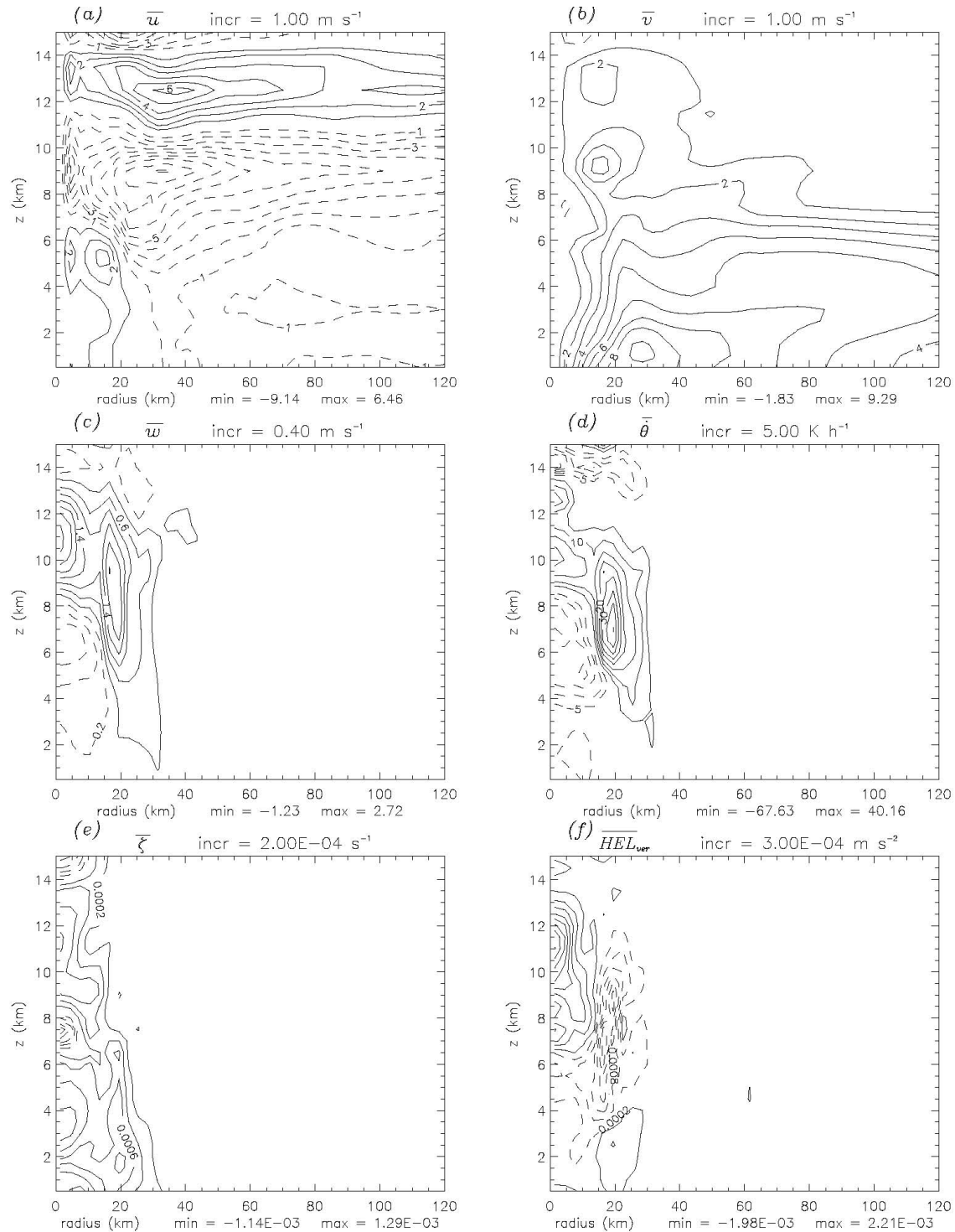


**Figure 14.** Azimuthal averages of (a) radial wind, (b) tangential wind, (c) vertical velocity, (d) diabatic heating rate, (e) relative vertical vorticity, and (f) vertical contribution of helicity at  $t = 16.5$  h from Experiment A2. The zero contour is omitted. Negative contours are dashed.

For the purpose of such analysis let us first describe briefly the whole evolution of TC vortex within Experiment A2. Our approach allows giving of quantitative estimations for a set of integral characteristics to pinpoint four milestones in tropical cyclone life cycle which correspond to formation of the secondary circulation (SC), tropical depression (TD), tropical storm (TS), and hurricane (H). Such estimates are given in Table 3. Maximal values that the integral characteristics reach over the whole experiment time can be of interest as well and also given in the Table.

The chosen set of integral characteristics includes total helicity integrated over the whole three-dimensional computational domain and its vertical and horizontal contributions,

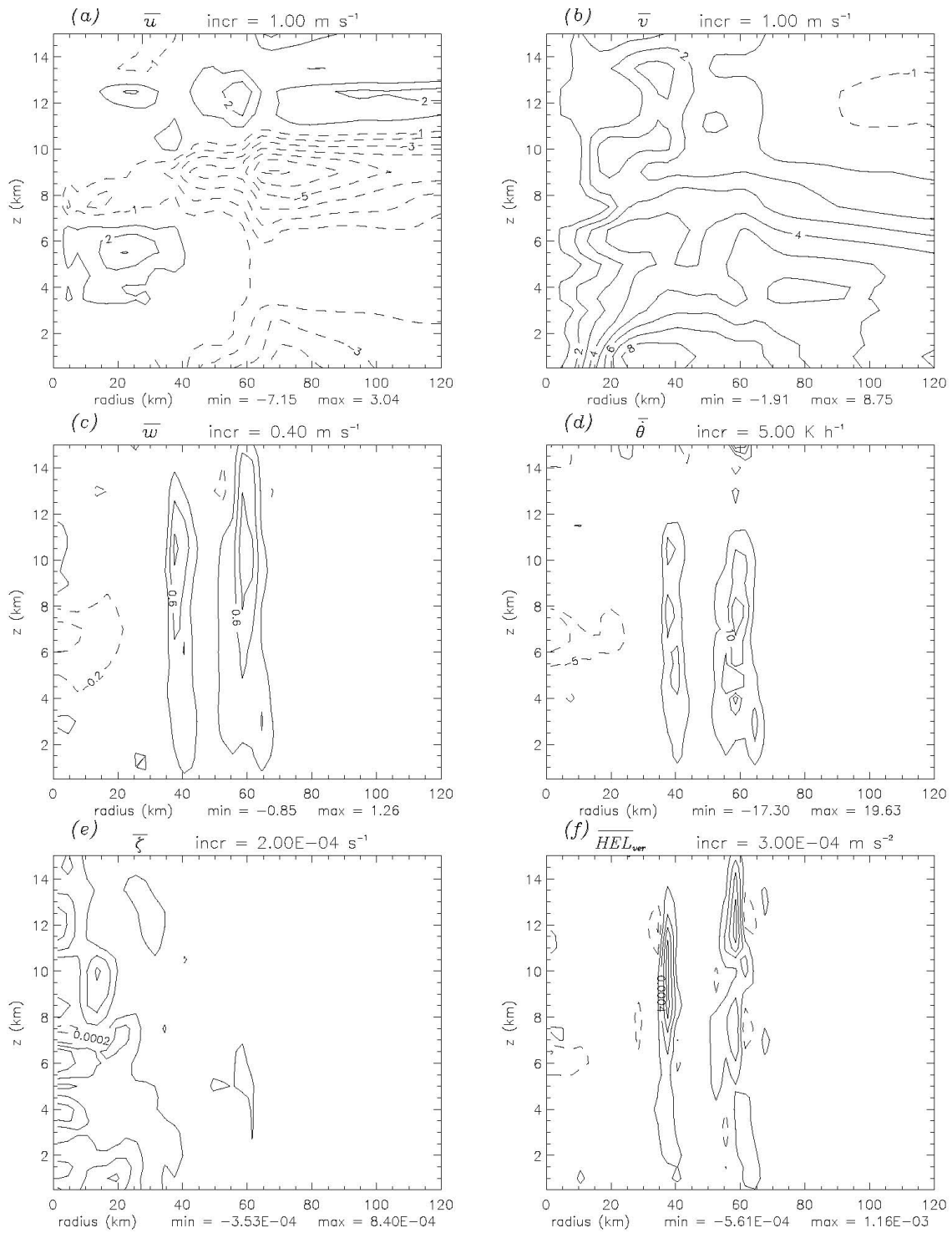


**Figure 15.** Azimuthal averages of (a) radial wind, (b) tangential wind, (c) vertical velocity, (d) diabatic heating rate, (e) relative vertical vorticity, and (f) vertical contribution of helicity at  $t = 18$  h from Experiment A2. The zero contour is omitted. Negative contours are dashed.

separately, the integral kinetic energy of the primary tangential circulation and of the secondary overturning one. We also calculate and use the maximum near-surface tangential wind to define a current stage of TC evolution.

It is worth recalling here the characteristic values of wind velocity for three stages of tropical cyclone strength. At the stage of tropical depression, the velocity of near surface tangential wind does not exceed  $17 \text{ m s}^{-1}$ , velocity values within  $17\text{--}33 \text{ m s}^{-1}$  correspond to the tropical storm, more than  $33 \text{ m s}^{-1}$  to the hurricane strength.

As it has been discussed in previous sections, the formation of the secondary circulation at  $t = 10\text{--}12 \text{ h}$  makes the nascent vortex energy-self-sustaining and may mark the genesis event. The maximal tangential wind at this stage is equal to  $6 \text{ m s}^{-1}$  and still located at middle levels, near  $z = 3\text{--}4 \text{ km}$ . The TD vortex formed during  $t = 16\text{--}18 \text{ h}$  has the maximum near-surface ( $z = 1 \text{ km}$ ) wind about  $9 \text{ m s}^{-1}$ . The consequently intensifying TD vortex reaches the TS intensity (the maximal tangential wind exceeds  $17 \text{ m s}^{-1}$ ) near  $t = 45 \text{ h}$  and H intensity, more than  $33 \text{ m s}^{-1}$ , about  $t = 56 \text{ h}$ . Within Experiment A2, the hurricane vortex attains its maximal tangential wind of approximately  $42 \text{ m s}^{-1}$  at  $t = 60\text{--}62 \text{ h}$ . Evolution of corresponding integral characteristics during 72 h of experiment time is shown in Figs. 10, 16, 17, and their values at different stages of TC intensity are presented in Table 3. It should be noted that values and graphics of total helicity and its horizontal contribution are near identical because the horizontal helicity is two orders of magnitude greater than the vertical contribution of helicity.

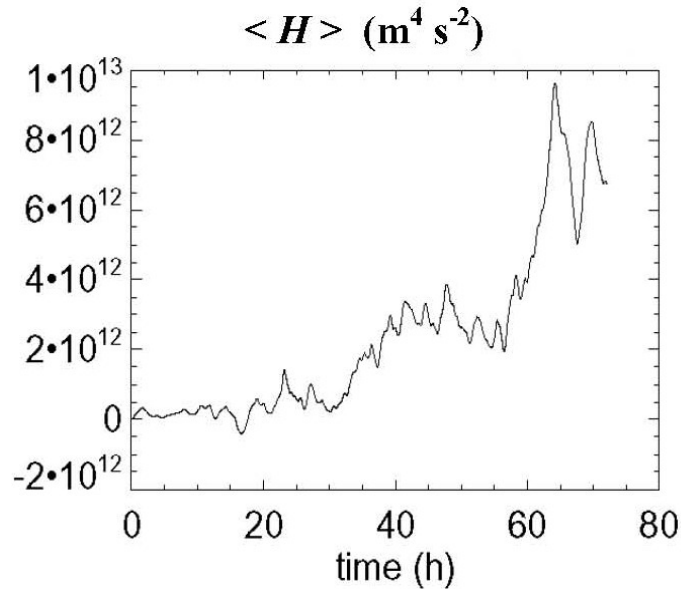


**Figure 16.** 72 hours evolution of total over 3D helicity in Experiment A2 “3 km”.

For our further analysis one more helical characteristic can be useful – mean helicity, which is the first statistical moment of turbulent helicity density field (2) and defined as the arithmetic mean.

To examine peculiarities of helicity generation in dependence on height, we calculated the mean values over the whole horizontal cross-sections at three different heights of 1, 4, and 7 km for the sum of two horizontal contributions of helicity and the vertical one, separately. As it has been already noted above, the sum of two horizontal contributions characterizes helicity generation by the vertical shear of horizontal wind (due to existing radial and tangential flows

over the whole troposphere layer) whilst the vertical contribution of helicity is generated by vortical convection.

Similarly to horizontal and vertical contributions of the total helicity over the whole three-dimensional computational domain, which we analyzed in previous sections, the mean values considered here are also about two orders of magnitude higher for horizontal contributions – Fig. 17.

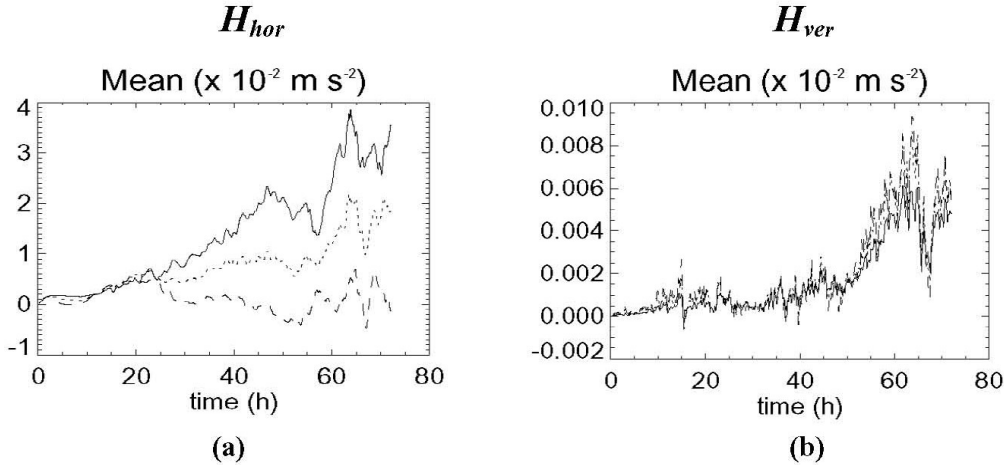


**Figure 17.** The first statistical moment evolution - mean over cross-sections - of horizontal (a) and vertical (b) helicity at different heights  $z = 1, 4$  (dotted), and  $7$  (dashed) km in Experiment A2 “3 km”.

The very first impression that comes when comparing two panels (a) and (b) in Fig. 17 is that we see very distinctly how different is horizontal helicity generation at different heights after  $t = 24\text{--}25$  h (Fig. 17a) and cannot find such pronounced difference of vertical helicity generation along the height of 1–7 km during all 72 hours of numerical experiment (Fig. 17b). Unlike the highest contribution of  $z = 1$  km horizontal helicity generation, the vertical helicity generation is somewhat weaker at the same lowest level than higher in the troposphere.

Thus, the quick conclusion follows that vortical convection contribution to helicity generation is very similar along 1–7 km in height. On the other hand, we can note a sharp increase in its generation at all three levels after  $t \sim 50$  h. Bear in mind a mechanism of vertical vorticity/helicity generation by tilting and stretching of horizontal components of vorticity, we may suggest a link to increased contribution of shear generated vorticity/helicity at that time.

Therefore, let us further discuss in more details what occurs with horizontal helicity generation.

During next few hours after the TD vortex formed at  $t = 16\text{--}18$  h, the near surface wind in TD was only gradually intensifying, exceeded  $10 \text{ m s}^{-1}$  at  $t = 21$  h and  $12 \text{ m s}^{-1}$  at  $t = 24\text{--}25$  h. This resulted in a corresponding increase in intensity of the primary circulation up to  $1.0 \times 10^{16} \text{ m}^5 \text{ s}^{-2}$  (Fig. 10). Such tangential flow intensification occurs at near-surface levels and inevitably suggests developing of significant vertical shear as well as direct interaction with the boundary layer.

Horizontal helicity “catches” such changed situation perfectly, when showing how differently it is now generated at different heights – Fig. 17a. Since  $t \sim 25$  h and everywhen ahead, the main generation of horizontal helicity occurs at  $h = 1$  km. Moreover, since this time and further, the contribution of the lowest level helicity generation is only positive (in our chosen frame of reference this corresponds to the dominate cyclonic tangential circulation) and persistently

increasing. This can only mean that vertical shear enters into play as the great contributor to helicity generation.

At the same time the secondary circulation is also strengthening due to working positive feedback which links both circulations. The kinetic energy of the secondary circulation grows up to  $0.5 \times 10^{16} \text{ m}^5 \text{ s}^{-2}$  till  $t = 25 \text{ h}$  (Fig. 10).

At this juncture we should explain a following and seeming surprisingly out of the increasing intensity tendency, a decrease of kinetic energy of both circulations after  $t = 25 \text{ h}$  (Fig. 10). It is necessary to note here a peculiarity that starts occurring nearly at the same time and is attributed to the specifics of numerical experiments (M06). Namely, the influence of diurnal cycle that can be traced in evolution of all integral characteristics. This is connected with time, when the RAMS model was initialized, and reveals in our results as weakening of convection due to decreasing ocean-air temperature difference during noon time (Golitsyn, 2009), every 24 hours.

On the other hand, this allows emphasizing the action of positive feedback between the primary and secondary circulation. Till  $t = 25 \text{ h}$  the primary tangential circulation becomes strong enough to support weakening secondary convective circulation through the feedback during a few hours, between  $t = 25\text{--}33 \text{ h}$  (Fig. 10), and provide further vortex intensification after this episode. A similar situation is observed again, 24 hours later.

Further development of large-scale vortex instability is realized as mutual intensification of the linked primary and secondary circulation. As total helicity evolution (Fig. 16) shows, the process is accompanied by a strong increase in the degree of linkage of vortex lines with time and, consequently, the increasing reflection asymmetry of atmospheric turbulence within the area of TC formation. This even stronger suppresses the energy transfer to dissipation scales and creates necessary conditions for further progress of upscale organization. The accumulated energy of rotating moist convective atmospheric turbulence is converted into the kinetic energy of large-scale vortex through the helical feedback.

Based on the above discussion, we may suggest discriminating of genesis and intensification stages in TC evolution by what is a leading mechanism of generation of the linkage of vortex lines, i.e. helicity. Moreover, it can be supported by quantitative data which are found to be sharply different for each of these stages.

Tropical cyclone genesis is developing under leading role of rotating deep convection, culminates in formation of the system-scale secondary circulation, which is found to be linked with the primary circulation via the positive helical feedback, and is completed when the full-fledged TD vortex evolves near  $t = 24\text{--}25 \text{ h}$ , which is characterized by near surface wind of  $12 \text{ m s}^{-1}$ . Total helicity values at this stage are relatively not high, yet, enough to create the system-scale linkage of circulations and initiate the large-scale vortex instability (Fig. 10, 16; Table 3). An intrinsic feature of this stage is that for both contributions of helicity, horizontal and vertical, generation occurs as accomplished by nearly equal contributions at different levels throughout 1–7 km of the troposphere height (Fig. 17a,b).

The second stage – TC intensification – commences within a flow configuration which contains a surface-concentrated tropical depression vortex that allows involving vertical shear in generation of helicity. Unlike initial hours characterized by weak vertical shear due to the initial MCV, now this mechanism produces horizontal vorticity/helicity of much greater intensity. After  $t \sim 25 \text{ h}$ , vertical shear, which increases due to intensifying TD, makes its decisive and persistently growing with time contribution to vorticity/helicity generation (Fig. 17a). When near  $t = 45 \text{ h}$ , the vortex reaches TS intensity, i.e. the maximum near-surface tangential wind exceeds  $17 \text{ m s}^{-1}$ , horizontal (as well as total) helicity becomes equal to  $3.3 \times 10^{12} \text{ m}^4 \text{ s}^{-2}$ , that is an order of magnitude higher than at the genesis stage – Table 3, Fig. 16.

However, the crucial role of rotating convection and VHTs stays the same during the whole TC evolution – producing the vertical vorticity from the horizontal components, amplifying it by

stretching and merging, and thereby, sustaining the linkage between the primary and secondary circulation and their mutual intensification through the helical feedback. Under increasing intensity of horizontal vorticity rich environment created by vertical shear, essentially stronger and larger VHTs, throughout the troposphere, 15–16 km in height, and up to 30 km in diameter develop (not shown). A sharp growth of convective activity after  $t \sim 50$  h is well traced in consistently increasing vertical helicity (Figs. 10, 17b) and leads to a hurricane vortex formation about  $t = 56$  h when the maximum tangential wind exceeds  $33 \text{ m s}^{-1}$ .

We may go even further and suppose that rotating convective structures are necessary elements to provide TC existence at all stages of its evolution because just they create and support the secondary circulation, produce and support the feedback between the primary and secondary circulation. It is also impossible to underestimate the role of deep moist convection in flow energetics, which allows transforming potential energy into the kinetic one and providing energy release due to phase transitions of water. Against the widespread opinion about negative impact of the vertical shear on TC development, we proposed how vorticity/helicity generated by shear can be used for TC intensification through VHTs activity. In mature hurricanes in a similar role may act meso-vortices in a eye-wall, as connectors and supporters of the primary and secondary circulations, by transforming shear generated horizontal vorticity/helicity into the vertical one.

*6.1.4. Effectiveness of helical feedback emphasized* After the helical feedback was initiated near  $t = 12$  h (i.e. when the linkage of primary and secondary circulation was formed), and until  $t = 60$ – $66$  h, when the maximal values of near-surface tangential wind and main integral characteristics were reached (Table 3, Figs. 10, 16), the kinetic energy of primary circulation was increased from  $0.45 \times 10^{16} \text{ m}^5 \text{ s}^{-2}$  up to  $2.9 \times 10^{16} \text{ m}^5 \text{ s}^{-2}$  whilst the kinetic energy of secondary circulation grew from  $0.05 \times 10^{16} \text{ m}^5 \text{ s}^{-2}$  up to  $2.3 \times 10^{16} \text{ m}^5 \text{ s}^{-2}$ . It is worth to note close enough intensity of both circulations in the hurricane strength vortex. This is quite different of that can be often find in meteorological literature about “a weak (?) enough yet energetically important secondary circulation” in a TC vortex. As we can see, it was this way only when the secondary circulation just formed (Table 3, Fig. 10), however, during all subsequent TC evolution the energy of secondary circulation was comparable with the energy of primary circulation by the order of magnitude.

*6.1.5. Digest of sensitivity experiments* Let us now briefly summarize results of other numerical experiments characterized by different initial conditions (Table 1).

Experiment C1 “No Vortex” is the simplest one amongst them for discussion because of that occurs during initial ten hours of this experiment was comprehensively analyzed in Section 5.1, and no flow organization was found at later times.

Three numerical experiments, B3, C3 and E1, were successful and resulted in formation of tropical depression vortices, all characterized by the mean near-surface tangential wind of 8–9  $\text{m s}^{-1}$ , however, formed at a different time in each experiment – 25–27 h (C3), 27–30 h (E1), and 45–50 h (B3). No intensification of the formed TDs up to TS and H strength vortices was observed in these experiments within 72 hours of simulation time. It should be noted, however, that in Expt. B3 after a delayed development of convection and TD formation only at  $t = 45$  h, all integral characteristics stayed increasing at the end of experiment,  $t = 72$  h, and demonstrated behavior, which was very similar to that in the middle of Expt. A2. Thus, TD intensification forecast in Expt. B3 might be as promising that further development is very likely. Similar is not true for two other experiments C3 and E1. Slowly intensifying TD vortex in Expt. C3 did not exceed  $9 \text{ m s}^{-1}$  intensity within 72 h, circulation stayed very asymmetric even at 72 h. In Expt. E1 no subsequent intensification of TD vortex observed through 72 h, till the end of experiment convection became very disorganized.

Nevertheless, examination of Expts. B3, C3 and E1 by using the same approach that was applied above for Expt. A2 allowed confirming all the tendencies found during formation of the secondary circulation and subsequent TD development.

The proposed approach for diagnosing the large-scale helical-vortex instability during TC formation was also tested by using a higher horizontal resolution of 2 km grid spacing. This was accomplished for Expt. A1 (M06), which is absolutely identical to Expt. A2, except horizontal grid increments. Despite some insignificant and being anticipated differences, all main findings and tendencies described above were confirmed.

## 7. Summary and conclusions

In the present paper we continued developing an unified view on tropical cyclone genesis and intensification, which is based on a fundamental idea of self-organization of moist convective atmospheric turbulence (Montgomery et al., 2006; Montgomery and Smith, 2010; Montgomery & Smith, 2011). We proposed an approach which features intrinsic helical nature of moist convective turbulence in the tropical atmosphere and allows quantifying the process of tropical cyclone formation on an unified methodological basis.

The main idea behind the approach is a specific topology of helical flows which are characterized by the linkage of vortex lines. Helicity is a well-known hydrodynamical invariant that quantifies the degree of such linkage and characterizes departure of the system from the mirror symmetry. As we discussed above, the linkage of vortex lines during tropical cyclone formation is generated by various physical mechanisms. At different stages of TC evolution the mechanisms participate by different contributions. Without specifying each mechanism, helicity allows quantifying their total influence on the global flow topology and identifying the break of the mirror symmetry as soon as it emerges in the examined flow. Therefore, we have chosen helicity examination as a perfect tool to try confirming the hypothesis on the turbulent vortex dynamo based on generating properties of small-scale helical atmospheric turbulence that was advanced as a possible mechanism for intensifying of large-scale vortex disturbances in planet atmospheres (see, our review in Section 2).

With all this in our mind, we were carrying out the present investigation.

Velocity fields resulted from a high resolution numerical simulation (Montgomery et al., 2006) were used to calculate helical and integral characteristics during a tropical cyclone formation. It was shown how non-zero total helicity is generated by moist convective atmospheric turbulence, which implies a new flow topology with linked vortex lines and the break of the mirror symmetry of turbulence.

On the basis of numerical analysis:

- It was demonstrated how the linkage of vortex lines (helicity) generation and amplification occurs on cloud convection and system scales by rotating convective updrafts and VHTs.
- The above investigation showed that the vertical contribution of total helicity could be proposed as a appropriate quantitative characteristic to trace evolution of rotating convection.
- The role of rotating deep convection in formation of the secondary overturning circulation in a nascent TC was emphasized.
- It was discovered that the secondary circulation was found to be linked with the primary tangential circulation through the positive energetic feedback. An emergence of such helical flow configuration turned an incipient mesoscale vortex to an integral helical system and made it energy-self-sustaining and, therefore, this was proposed to be considered as a TC genesis event.
- Surface-concentrated warm-core tropical depression (TD) vortex was diagnosed a few hours later the genesis event as a result of evolving large-scale vortex instability.
- A quantitative illustration was presented of how the positive energetic feedback between

the circulations worked providing the vortex intensification consequently through TD and TS intensity up to hurricane strength.

- It was proposed to distinguish tropical cyclone genesis and intensification stages by what is a leading mechanism contributing to helicity generation – moist convection or vertical shear.

- The crucial role of vertical shear was suggested in TC intensification through its interaction with VHTs, which act by gaining shear generated horizontal vorticity, transforming it into the vertical one and amplifying it by stretching and merging.

- Based on the obtained results, a special role of VHTs was suggested as generators of helicity and natural connectors between the primary and secondary circulation during the whole TC evolution.

- All above reported findings were quantified by a set of integral helical and energetic characteristics.

Further tests are encouraged through diagnoses of high resolution operational and cloud models, examination of other scenarios for incipient storms, especially, under shear environment to further clarify and quantify its positive (!) role in TC formation.

In order to summarize, it would be appropriate to mention the so-called “Marsupial Paradigm” advanced recently (Dunkerton et al., 2009) as a series of hypotheses on tropical cyclogenesis in a critical layer of tropical easterly waves, as well as based on it the “Marsupial Pouch Tracking” (Wang et al., 2009). This approach tested in the field experiment PREDICT (Pre-Depression Investigation of Cloud-systems in the Tropics) (Montgomery et al., 2012) allows high accuracy predicting of TC genesis location, namely, up to 3 days and with an error less than 200 km.

Thus, about tropical cyclogenesis the Marsupial Paradigm answers a question “WHERE ?” – within a “Pouch”. Analysis of helicity can answer another important question “WHEN ?” – at that time when the primary and secondary circulations become linked by vortical hot towers making the nascent vortex helical and energy-self-sustaining.

Following the above summary, useful practical recommendations are evident about combining the Marsupial Pouch Tracking with analysis of helicity in order to localize maximally a space area where helical approach should be applied on a high resolution space grid.

## Acknowledgments

This work based on high-resolution atmospheric data for “A Vortical Hot Tower Route to Tropical Cyclogenesis” by M.T. Montgomery et al. (2006) is a contribution to our collaborative efforts with Michael Montgomery (Naval Postgraduate School, Monterey, CA; NOAA/Hurricane Research Division, Miami, FL, USA) aimed at introducing the analysis of helicity in tropical cyclone investigations. I am deeply grateful to Professor H.-K. Moffatt for his invitation to participate in the INI Programme on Topological Dynamics and important discussions. I thank the co-organizers of the Programme and Isaac Newton Institute for hospitality. The work was supported by the Russian Foundation for Basic Research, Grant 10-05-00100-a, and the Russian Academy of Science, Programme EMMPU 12-T-1-1008.

## References

- Biferale, L., Musacchio, S., and Toschi, F.: Inverse energy cascade in three-dimensional isotropic turbulence, *Phys. Rev. Lett.* 108, 164501, 2012. doi:10.1103/PhysRevLett.108.164501
- Bister, M. and Emanuel, K.: The genesis of Hurricane Guillermo: TEXMEX analyses and a modeling study, *Mon. Wea. Rev.*, 125, 2662-2682, 1997.
- Bogatyrev, G. P., Kolesnichenko I. V., Levina G. V., and Sukhanovsky A. N.: Laboratory model

- of generation of a large-scale spiral vortex in a convectively unstable rotating fluid, *Izv. Atmos. Oceanic Phys.*, 42(4), 423–429, 2006.
- Bogner, P. B., Barnes, G. M., and Franklin, J. L.: Conditional instability and shear for six hurricanes over the Atlantic Ocean, *Wea. Forecasting*, 15, 192–207, 2000.
- Boubnov, B. M.: Thermal structure and turbulization of tornado-like vortices from a localized heat source over a rotating disk, *Izv. Atmos. Ocean. Phys.*, 33, 399–406, 1997a.
- Boubnov, B. M.: Convection driven by local heating in a slowly rotating fluid, *Izv., Atmos. Ocean. Phys.* 33, 736–743, 1997b.
- Braun, S. A., Montgomery, M. T., Mallen, K. J., and Reasor, P.D.: Simulation and interpretation of the genesis of tropical storm GERT (2005) as part of the NASA tropical cloud systems, *J. Atmos. Sci.*, 2010, in press.
- Chandrasekhar, S.: *Hydrodynamic and hydromagnetic stability*, Clarendon Press, Oxford, 1961.
- Davies-Jones, R. P., Burgess, D., and Foster, M.: Test of helicity as a tornado forecast parameter, in: *Preprints of the 16th Conference on Severe Local Storms*, Kananaskis Park, AB, Canada, Amer. Meteor. Soc., 588–592, 1990.
- Davis, C. A. and Bosart, L. F.: Numerical simulation of the genesis of Hurricane Diana (1984), Part I: Control simulation, *Mon. Weather Rev.*, 129, 1859–1881, 2001.
- Droegemeier, K. K., Lazarus, S. M., and Davies-Jones, R. P.: The influence of helicity on numerically simulated convective storms, *Mon. Weather. Rev.*, 121, 2005–2029, 1993.
- Dunion, J. P. and Velden, C.S.: The impact of the Saharan air layer on Atlantic tropical cyclone activity, *Bull. Amer. Meteor. Soc.*, 85, 353–365, 2004.
- Dunkerton, T. J., Montgomery, M. T., and Wang, Z.: Tropical cyclogenesis in a tropical wave critical layer: easterly waves, *Atmos. Chem. Phys.*, 9, 5587–5646, 2009.
- Emanuel, K.: Tropical Cyclones, *Annu. Rev. Earth Planet. Sci.*, 31, 75–104, 2003.
- Fang, J. and Zhang, F.: Initial development and genesis of Hurricane Dolly (2008), *J. Atmos. Sci.*, 67, 655–672, 2010
- Fortov, V. E., Ivanov, M. F., Ivlev, A. V., Gnedin, Yu. N., and Klumov, B. A.: Collision of comet Shoemaker-Levy 9 with Jupiter: what did we see, *Usp. Fiz. Nauk*, 166, pp. 391–422, 1996 (in Russian). (Engl. transl. *Phys. Usp.* 39, 363–392 (1996)).
- Frisch, U.: *Turbulence: the legacy of A.N. Kolmogorov*, Cambridge University Press, Cambridge, UK, 1995.
- Frisch, U., She, Z. S., and Sulem, P. L.: Large-scale flow driven by the anisotropic kinetic alpha effect, *Physica D*, 28, 382–392, 1987.
- Gershuni, G. Z. and Zhukhovitsky, E. M.: *Convective stability of incompressible fluid*, Nauka, Moscow, 1972 (in Russian). (Engl. transl. Keterpress, Jerusalem, 1976.)
- Golitsyn, G. S.: Tropical cyclones and polar lows: velocity, size, and energy scales, and relation to the 26<sup>0</sup>C cyclone origin criteria, *Adv. Atmos. Sci.*, 26(3), 585–598, 2009, doi: 10.1007/s00376-009-0585-z
- Gray, W. M.: Tropical cyclone genesis, *Tropical cyclone genesis*. Dept. of Atmos. Sci. Paper No. 234, Colo. State. Univ., Fort Collins, CO, 121 pp., 1975.
- Gray, W. M.: Hurricanes: their formation, structure, and likely role in the tropical circulation, in: *In Meteorology Over the Tropical Oceans*, Shaw, D. B. (Ed.): R. Meteorol. Soc., Reading, UK, 155–218, 1979.
- Gray, W. M.: The formation of tropical cyclones, *Meteorol. Atmos. Phys.*, 67, 37–69, 1998.
- Hendricks, E. A., Montgomery, M. T., and Davis, C. A.: The role of “vortical” hot towers in the formation of tropical cyclone Diana (1984), *J. Atmos. Sci.*, 61, 1209–1232, 2004.

- Hide, R.: A note on helicity, *Geophys. (& Astrophysical- after 1977) Fluid Dyn.*, 7, 157–161, 1976.
- Hide, R.: Superhelicity, helicity and potential vorticity, *Geophys. Astrophys. Fluid. Dyn.*, 48, 69–78, 1989.
- Hide, R.: Helicity, superhelicity and weighted relative potential vorticity: Useful diagnostic pseudoscalars?, *Q. J. R. Meteor. Soc.*, 128, 1759–1762, 2002.
- Holton, J. R.: An introduction to dynamic meteorology, Academic Press, London, 2004.
- Ivanov, M. F., Galburt, V. A., and Fortov, V. E.: On possible mechanism of large-scale disturbances formation in Jovian atmosphere initiated by a fall of comet Shoemaker-Levy 9 fragments, *Z. Eksp. Teor. Fiz. Letters*, 63, 773–777, 1996 (in Russian). (Engl. transl. *Letters to JETP*, 63, 813–817, 1996.)
- Johns, R. H. and Doswell III C. A.: Severe local storms forecasting, *Wea. Forecasting*, 7, 588–612, 1992.
- Jordan, C. L.: Mean soundings for the West Indies area, *J. Meteor.*, 15, 91–97, 1958.
- Kakar, R., Goodman, M., Hood, R., and Guillory, A.: Overview of the Convection and Moisture Experiment (CAMEX), *J. Atmos. Sci.*, 63, 5–18, 2006.
- Kolmogorov, A. N.: The local structure of turbulence in incompressible viscous fluid for very large Reynolds number, *Dokl. Akad. Nauk SSSR*, 30, 9–13, 1941 (in Russian). Reprinted in *Proc. R. Soc. Lond., Ser. A* 434, 9–13, 1991.
- Koprov, B. M., Koprov, V. M., Ponomarev, V.M., and Chkhetiani, O.G.: Experimental studies of turbulent helicity and its spectrum in the atmospheric boundary layer, *Dokl. Physics*, 50, (8), 417–422, 2005.
- Kurgansky, M. V.: Generation of helicity in a moist atmosphere, *Izv. Atmos. Oceanic Phys.*, 29(4), 444–448, 1993.
- Kurgansky, M. V.: Vorticity generation in a moist atmosphere, *Izv. Atmos. Oceanic Phys.*, 34(2), 156–161, 1998.
- Kurgansky, M. V.: Vorticity genesis in the moist atmosphere, *Phys. Chem. Earth Part B*, 24, 8, 959–961, 1999.
- Kurgansky, M. V.: *Adiabatic Invariants in Large-Scale Atmospheric Dynamic*, Taylor and Francis, London and New York, 2002.
- Levich, E. and Tzvetkov, E.: Helical cyclogenesis, *Phys. Lett. A*, 100, 53–56, 1984.
- Levich, E. and Tzvetkov, E.: Helical inverse cascade in three-dimensional turbulence as a fundamental dominant mechanism in mesoscale atmospheric phenomena, *Phys. Rep.*, 128, 1–37, 1985.
- Levina, G. V., Moiseev, S. S., and Rutkevich, P. B.: Hydrodynamic alpha-effect in a convective system, in: *Nonlinear Instability, Chaos and Turbulence*, vol. 2, *Adv. Fluid Mech. Series*, Debnath, L. and Riahi, D. N. (Eds.): WITPress, Southampton, Boston, 111–162, 2000.
- Levina, G.V., Burylov, I.A., Firulyov, A.V., and Shestakova, L.V.: Helical-Vortex Instability in a Convectively Unstable Fluid: Origin and Numerical Simulation, Russian Academy of Sciences, Institute of Continuous Media Mechanics, Perm, Preprint ICMM UB RAS, 160, 2004.
- Levina, G. V.: Parameterization of helical turbulence in numerical models of intense atmospheric vortices, *Dokl. Earth Sci.*, 411A, (9), 1417–1421, 2006a.
- Levina, G. V. and Burylov, I. A.: Numerical simulation of helical-vortex effects in Rayleigh-Bénard convection, *Nonlin. Processes Geophys.*, 13, 205–222, 2006b.

- Levina, G. V. and Montgomery, M. T.: A first examination of the helical nature of tropical cyclogenesis, *Doklady Earth Sciences*, 434, Part 1, 1285–1289, 2010.
- Levina, G. V. and Montgomery, M. T.: Helical scenario of tropical cyclone genesis and intensification, *J. Phys.: Conf. Ser.*, 318, 072012, 2011. doi:10.1088/1742-6596/318/7/072012
- Lilly, D. K.: The structure, energetics, and propagation of rotating convective storms. Part II: Helicity and storm stabilization, *J. Atmos. Sci.*, 43, 126–140, 1986.
- Lilly, D. K.: Numerical prediction of thunderstorms ? Has its time come? *Quart. J. Roy. Meteor. Soc.*, 116, 779-798, 1990.
- McCaul, E. W., Jr.: Observations of the Hurricane “Danny” tornado outbreak of 16 August 1985, *Mon. Wea. Rev.*, 115, 1206-1223, 1987.
- McCaul, E. W., Jr.: Buoyancy and shear characteristics of hurricane tornado environments, *Mon. Wea. Rev.*, 119, 1954-1978, 1991.
- McCaul, E. W., Jr. and Weisman, M. L.: Simulations of shallow supercell storms in landfalling hurricane environments, *Mon. Wea. Rev.*, 124, 408-429, 1996.
- Mininni, P. D., Alexakis, A., and Pouquet, A.: Scale interactions and scaling laws in rotating flows at moderate Rossby numbers and large Reynolds numbers, *Phys. Fluids*, 21, 015108, 2009. doi:10.1063/1.3064122
- Mininni, P. D. and Pouquet, A.: Helicity cascades in rotating turbulence, *Phys. Rev. E* 79, 026304, 2009. doi:10.1103/PhysRevE.79.026304
- Mininni, P. D. and Pouquet, A.: Rotating helical turbulence. Part I. Global evolution and spectral behavior, *Phys. Fluids*, 22, 035105, 2010. doi:10.1063/3358466
- Mininni, P. D. and Pouquet, A.: Helical rotating turbulence. Part II. Intermittency, scale invariance and structures, *Phys. Fluids*, 22, 035106, 2010. doi:10.1063/3358471
- Moffatt, H. K.: The degree of knottedness of tangled vortex lines, *J. Fluid Mech.*, 35, 117–129, 1969.
- Moffatt, H. K.: *Magnetic Field Generation in Electrically Conducting Fluids*, Cambridge University Press, Cambridge, 1978.
- Moffatt, H. K. and Tsinober, A.: Helicity in laminar and turbulent flow, *Ann. Rev. Fluid Mech.*, 24, 281–312, 1992.
- Moiseev, S. S., Sagdeev, R. Z., Tur, A. V., Khomenko, G. A., and Yanovsky, V. V., A theory of large-scale structure origination in hydrodynamic turbulence, *Z. Eksp. Teor. Fiz.*, 85, 1979–1987, 1983 (in Russian). Engl. transl. *Sov. Phys. JETP*, 58, 1149–1157, 1983a.
- Moiseev, S. S., Sagdeev, R. Z., Tur, A. V., Khomenko, G. A., and Shukurov, A. M.: Physical mechanism of amplification of vortex disturbances in the atmosphere, *Dokl. Akad. Nauk SSSR*, 273, 549–553, 1983 (in Russian). Engl. transl. *Sov. Phys. Dokl.*, 28, 925–928, 1983b.
- Moiseev, S. S., Rutkevich, P. B., Tur, A. V., and Yanovski, V. V.: Vortex dynamos in a helical turbulent convection, *Z. Eksp. Teor. Fiz.*, 94, 144–153, 1988 (in Russian). Engl. transl. *Sov. Phys. JETP*, 67, 294–299, 1988.
- Molinari, J. and Vollaro, D.: Extreme helicity and intense convective towers in Hurricane Bonnie, *Mon. Weather. Rev.*, 136, 4355–4372, 2008.
- Molinari, J. and Vollaro, D.: Distribution of helicity, CAPE, and shear in tropical cyclones, *J. Atmos. Sci.*, 67, 274–284 2010. doi: 10.1175/2009JAS3090.1
- Monin, A. S. and Yaglom, A. M.: *Statistical Fluid Mechanics*, MIT Press, vol.2, ed. J.Lumley, Cambridge, MA, 1975.
- Montgomery, M. T., Nicholls, M. E., Cram, T. A., and Saunders A. B.: A vortical hot tower route to tropical cyclogenesis, *J. Atmos. Sci.*, 63, 355–386, 2006.

- Montgomery, M. T., Nguyen, S. V., and Smith, R. K.: Do tropical cyclones intensify by WISHE? *Q. J. R. Meteor. Soc.*, 135, 1697–1714, 2009.
- Montgomery, M. T. and Smith, R. K.: Tropical-Cyclone Formation: Theory and Idealized modeling, Topic 2.1 of WMO/CAS/WWW Seventh International Workshop on Tropical Cyclones. Workshop held in November 2010 in La ReUnion. J. Kepert and J. Chan. Editors. 23 pp., 2010.
- Montgomery, M. T. and Smith, R. K.: Paradigms for tropical-cyclone intensification, *Q. J. R. Meteor. Soc.*, 137, 2011 (submitted).
- Michael T. Montgomery, Cristopher Davis, Timothy Dunkerton, Zhuo Wang, Christopher Velden, Ryan Torn, Sharanya J. Majumdar, Fuqing Zhang, Roger K. Smith, Lance Bosart, Michael M. Bell, Jennifer S. Haase, Andrew Heymsfield, Jorgen Jensen, Teresa Campos, and Mark A. Boothe: The pre-depression investigation of cloud-systems in the tropics (PREDICT) experiment. Scientific basis, new analysis tools, and some first results, *Bull. Amer. Meteor. Soc.*, 93, 153–172, 2012.
- Nguyen, S. V., Smith, R. K., and Montgomery, M. T.: Tropical-cyclone intensification and predictability in three dimensions, *Q. J. R. Meteor. Soc.*, 134, 563–582, 2008.
- Nolan, D. S.: Evaluating environmental favorableness for tropical cyclone development with the method of point-downscaling, *J. Adv. Model. Earth Syst.*, 3, M08001, doi:10.1029/2011MS000063, 2011.
- Obukhov, A. M.: Spectral energy distribution in a turbulent flow, *Izv. Akad. Nauk SSSR, Ser. Geogr. Geofiz.*, 5 (4–5), 453–466, 1941 (in Russian).
- Parker, E. N.: *Cosmical Magnetic Fields*, Clarendon, Oxford, 1979.
- Pouquet, A. and Mininni, P. D.: The interplay between helicity and rotation in turbulence: implications for scaling laws and small-scale dynamics, *Phil. Trans. R. Soc. A*, 368, 1635–1662, 2010. doi:10.1098/rsta.2009.0284
- Rasmussen, E. N. and Blanchard, D. O.: A baseline climatology of sounding-derived supercell and tornado forecast parameters, *Wea. Forecasting*, 13, 1148–1164, 1998.
- Reasor, P. D., Montgomery, M. T., and Grasso, L. D.: A new look at the problem of tropical cyclones in vertical shear flow: Vortex resiliency, *J. Atmos. Sci.*, 60, 97–116, 2004.
- Reasor, P. D., Montgomery, M. T., and Bosart, L.: Mesoscale observations of the genesis of Hurricane Dolly (1996), *J. Atmos. Sci.*, 62, 3151–3171, 2005.
- Reed, R. J., Norquist D. C., and Recker, E. E.: The structure and properties of African wave disturbances as observed during phase III of GATE, *Mon. Wea. Rev.*, 105, 317–333, 1977.
- Riehl, H. and Malkus, J. S.: On the heat balance in the equatorial trough zone, *Geophysica*, 6, 503–538, 1958.
- Ritchie, E. A. and Holland, G. J.: Scale interactions during the formation of Typhoon Irving, *Mon. Wea. Rev.*, 125, 1377–1396, 1997.
- Rutkevich, P. B.: Equation for vortex instability caused by convective turbulence and the Coriolis force, *J. Exp. Theor. Phys.*, 77, 933–938, 1993.
- Shin, S. and Smith, R. K.: Tropical-cyclone intensification and predictability in a minimal three-dimensional model, *Q. J. R. Meteorol. Soc.*, 134, 1661–1671, 2008.
- Simpson, J., Ritchie, E. A., Holland, G. J., Halverson, J., and Stewart, S.: Mesoscale interactions in tropical cyclone genesis, *Mon. Wea. Rev.*, 125, 2643–2661, 1997.
- Steenbeck, M., Krause, F., and Rädler, K.-H.: Zur Berechnung der mittleren Lorentz-Feldstärke  $\mathbf{v} \times \mathbf{B}$  für ein elektrisch leitendes Medium in turbulenter, durch Coriolis-Kräfte beeinflusster Bewegung, *Z. Naturforsch., A: Phys. Sci.* 21, 369–376, 1966.

- Wang, Z., Montgomery, M.T., and Dunkerton, T. J.: A dynamically-based method for forecasting tropical cyclogenesis location in the Atlantic sector using global model products, *Geophys. Res. Lett.*, 36, L03801, 2009.
- Weisman, M. L. and Rotunno, R.: The use of vertical wind shear versus helicity in interpreting supercell dynamics, *J. Atmos. Sci.*, 57, 1452-1472, 2000.
- Wikipedia, the Free Encyclopedia, [http://www.en.wikipedia.org/wiki/Hot\\_tower](http://www.en.wikipedia.org/wiki/Hot_tower)
- Zeldovich, Y. B., Ruzmaikin, A. A., and Sokoloff, D. D.: *Magnetic Fields in Astrophysics*, Gordon & Breach, London, 1983.

**Table 1.** RAMS numerical experiments [M06] analyzed in this work

No.	Name of experiment	Max $v$ ( $\text{m} \cdot \text{s}^{-1}$ ) at $z=4$ km	Description of experiment
A1	Control	6.6	$\Delta x = \Delta y = 2$ km, SST <sup>1</sup> = 29°C. Metamorphosis to surface vortex successful. Becomes miniature tropical cyclone by approximately 60 h. Mean near-surface tangential wind $\approx 12 \text{ m} \cdot \text{s}^{-1}$ at 24 h, and $46 \text{ m} \cdot \text{s}^{-1}$ at 72 h.
A2	3 km	6.6	$\Delta x = \Delta y = 3$ km, SST = 29°C. Metamorphosis to surface vortex successful. Mean near-surface tangential wind $\approx 13 \text{ m} \cdot \text{s}^{-1}$ at 24 h, and $46 \text{ m} \cdot \text{s}^{-1}$ at 72 h.
B3	CAPE-less <sup>2</sup> (3 km)	6.6	$\Delta x = \Delta y = 3$ km, SST = 29°C. Low-level moisture decreased by $2 \text{ g} \cdot \text{kg}^{-1}$ . Metamorphosis successful, but slower rate of development. Mean near-surface tangential wind $\approx 9 \text{ m} \cdot \text{s}^{-1}$ at 48 h.
C1	No Vortex	—	$\Delta x = \Delta y = 3$ km, SST = 29°C. No initial vortex. No surface development whatsoever.
C3	Weak Vortex	5.0	$\Delta x = \Delta y = 3$ km, SST = 29°C. Metamorphosis successful, but slower rate of development. Mean near-surface tangential wind $\approx 9 \text{ m} \cdot \text{s}^{-1}$ at 72 h. Circulation very asymmetric even at 72 h.
E1	Zero Coriolis	6.6	$\Delta x = \Delta y = 3$ km, SST = 29°C. Coriolis parameter set to zero ( $f = 0$ ). Metamorphosis successful. Develop surface-concentrated vortex as in A1, but no subsequent intensification observed through 72 h.

<sup>1</sup> SST - Sea Surface Temperature

<sup>2</sup> Convective Available Potential Energy

<b>Experiment</b>	<b>Total Helicity &lt; <math>H</math> &gt;</b>
<b>A2</b>	<b><math>3.3 \times 10^{11} \text{ m}^4 \text{ s}^{-2}</math></b>
<b>B3</b>	<b><math>2.0 \times 10^{11} \text{ m}^4 \text{ s}^{-2}</math></b>
<b>C1</b>	<b><math>2.0 \times 10^{10} \text{ m}^4 \text{ s}^{-2}</math></b>
<b>C3</b>	<b><math>2.5 \times 10^{11} \text{ m}^4 \text{ s}^{-2}</math></b>
<b>E1</b>	<b><math>3.5 \times 10^{11} \text{ m}^4 \text{ s}^{-2}</math></b>

**Table 2.** The highest values of Total Helicity attained due to the initial break of mirror symmetry generated by the initial conditions.

<b>Expt.</b>	<b>Time h</b>	<b>Event</b>	<b>Maximal Tangential Wind <math>\text{m s}^{-1}</math></b>	<b>Vertical Helicity <math>\langle H_{ver} \rangle</math> <math>\text{m}^4 \text{s}^{-2}</math></b>	<b>Horizontal Helicity <math>\langle H_{hor} \rangle</math> <math>\text{m}^4 \text{s}^{-2}</math></b>	<b>Kinetic Energy <math>\langle E^P \rangle</math> <math>\text{m}^5 \text{s}^{-2}</math></b>	<b>Kinetic Energy <math>\langle E^S \rangle</math> <math>\text{m}^5 \text{s}^{-2}</math></b>
<b>A2</b>	10-12	<b>SC</b>	6 (z=3-4km)	$1.5 \times 10^{10}$	$0.4 \times 10^{12}$	$0.45 \times 10^{16}$	$0.05 \times 10^{16}$
	16-18	<b>TD</b>	9	$-1.6 \times 10^{10}$	$-0.4 \times 10^{12}$	$0.7 \times 10^{16}$	$0.35 \times 10^{16}$
	45	<b>TS</b>	17.2	$3.0 \times 10^{10}$	$3.3 \times 10^{12}$	$1.7 \times 10^{16}$	$1.0 \times 10^{16}$
	56	<b>H</b>	33.4	$3.7 \times 10^{10}$	$3.5 \times 10^{12}$	$2.0 \times 10^{16}$	$1.1 \times 10^{16}$
	60-66	<b>Max</b>	42	$9.8 \times 10^{10}$	$9.8 \times 10^{12}$	$2.9 \times 10^{16}$	$2.3 \times 10^{16}$

**Table 3.** Integral values which characterize secondary circulation (SC), tropical depression (TD), tropical storm (TS), and hurricane (H) formation. **Max** – maximal values over the whole experiment time.